MARMARA UNIVERSITY
FACULTY OF ENGINEERING

Passive Isolator Design and Vibration Damping of EO/IR Gimbal to be Used in UAVs

Mehmet Taha GÖRMÜŞ, Bilal Faruk ADIN

GRADUATION PROJECT REPORT
Department of Mechanical Engineering

Supervisor
Prof. Dr. Paşa YAYLA

ISTANBUL, 2022

MARMARA UNIVERSITY
FACULTY OF ENGINEERING

Passive Isolator Design and Vibration Damping of EO/IR Gimbal to be Used in UAVs

by

Mehmet Taha GÖRMÜŞ, Bilal Faruk ADIN

JUNE 15, 2022, Istanbul

SUBMITTED TO THE DEPARTMENT OF MECHANICAL ENGINEERING IN PARTIAL FULFILLMENT OF THE REQUIREMENTS FOR THE DEGREE

OF

BACHELOR OF SCIENCE

AT

MARMARA UNIVERSITY

Signature of Author(s) .....

Department of Mechanical Engineering

Certified By .....

Project Supervisor, Department of Mechanical Engineering

Accepted By .....

Head of the Department of Mechanical Engineering

ACKNOWLEDGEMENT

First of all, we would like to thank our supervisor, who is Prof. Dr. Paşa YAYLA ,for the valuable guidance from before the starting fall semester to the end of our studies advice on preparing this thesis , and giving us moral, idea , and material support at every stage of our studies.

We also would like to thank TÜBİTAK for supporting our project within the scope of the 2209-A University Students Research Projects Support Program, which provides financial resource and material for us. In addition, we also would like to thank Kadir Doğan, who is the founder of the Blitz Systems for giving suggestions for our work on this subject.

June,2022

Mehmet Taha GÖRMÜŞ & Bilal Faruk ADIN

CONTENTS

ÖZET

İnsansız hava araçlarında (İHA) kullanılan gözetleme sistemlerinin yakaladığı görüntülerin kalitesini etkileyen önemli faktörlerden biri de hava aracından gimbala iletilen titreşimlerdir. Bu tez kapsamında, mini insansız hava aracında kullanılan iki eksenli elektro-optik gimbal için pasif titreşim sönümleyici tasarımı yapılmıştır. Öncelikle İHA'da meydana gelebilecek titreşimlerin anlaşılması için literatür çalışması yapılmış daha sonra da pasif sönümleyiciler için literatür incelenmiştir. Farklı yöntemler arasından yay-damper sistemi seçilerek platformdan gelen harmonik titreşimi tek eksende sönümleyen tasarım analitik yöntemle yapılmıştır. Ayrıca bu sönümleyici sistemi içerisinde bulunduran 'Pan Yoke' isimli parçanın CAD program ile tasarımı yapılarak Ansys modal analizi ile doğal frekans değerleri kontrol edilmiştir. Hava aracından gimbala iletilen titreşimin frekansı ile tasarımı yapılan parçanın doğal frekansının 150 Hz civarında birbirine yakın olduğu saptanmıştır. Bu parçanın doğal frekans değerleri çeşitli tasarım değişiklikleri ve topoloji optimizasyonu ile değiştirilerek parçanın rezonansa girmesi önlenmiştir.

Anahtar Kelimeler: Pasif titreşim izolatörleri, Harmonik titreşim, İnsansız hava araçları, Elektro-optik gimbal, Ansys modal analiz, Topoloji optimizasyonu

ABSTRACT

One of the important factors affecting the quality of the images captured by the surveillance systems used in unmanned aerial vehicles (UAV) is the vibrations transmitted from the aircraft to the gimbal. Within the scope of this thesis, a passive vibration isolation system design has been made for the two-axis electro-optical gimbal used in the mini unmanned aerial vehicle. First of all, a literature study was conducted to understand the vibrations that may occur in the UAV, and then the literature for passive vibration isolators were examined. By choosing the spring-damper system among different methods, the design that isolates the harmonic vibration coming from the platform in a single axis has been made with analytical method. In addition, the part named 'Pan Yoke', which contains this damper system, was designed with a CAD program and natural frequency values were checked with Ansys modal analysis. It has been determined that the frequency of the vibration transmitted from the air vehicle to the gimbal, and the natural frequency of the designed part are close to each other, around 150 Hz. The natural frequency values of this part have been changed with various design changes and topology optimization to prevent the part from resonating.

Keywords: Passive vibration isolators, Harmonic vibration, Unmanned aerial vehicles, Electro-optical gimbal, Ansys modal analysis, Topology optimization

SYMBOLS

ω	: angular velocity, rad/s
K_B	: bergstrasser factor
c_c	: critical damper coefficient, Ns/m
c	: damper coefficient, Ns/m
ζ	: damping ratio
F_{eq}	: external excitation force, N
n_s	: factor of safety
L_0	: free length, mm
r	: frequency ratio
M	: magnification factor
m	: mass, kg
ω_n	: natural frequency, rad/s
N_a	: number of active coils
N_t	: number of total coils
D	: outer diameter, mm
$\emptyset$	: phase angle, rad
p	: pitch, mm
S	: shape factor
G	: shear modulus, GPa
τ	: shear stress, MPa
K_s	: shear-stress correction factor
L_s	: solid length, mm
C	: spring index
k	: spring rate, N/m
Δ_{st}	: static deflection, mm

ABBREVIATIONS

CAD : Computer Aided Design
DFT : Discrete Fourier Transform
EO : Electro-Optical
FEA : Finite Element Analysis
FFT : Fast Fourier Transform
IR : Infrared
PSD : Power Spektrum Density
SAR : Synthetic Aperture Radar
SDOF : Single Degree-of-Freedom
UAS : Unmanned Aircraft Systems
UAV : Unmanned Aerial Vehicle

LIST OF FIGURES

LIST OF TABLES

INTRODUCTION

1.1 Overview

Unmanned Aerial Vehicle (UAV) projects, which have become popular in the world and Turkey in recent years, are carried out by different companies worldwide for military and civilian purposes. Turkey has taken its place among the leading countries of this technological trend and has produced UAVs in many different classes. Since the main purpose of these unmanned aerial vehicles is observation, many useful loads such as Electro-Optical (EO) and Infrared (IR) cameras and Synthetic Aperture Radar (SAR) systems are being developed worldwide for this purpose. However, while there are a few imaging system manufacturers suitable for UAV projects above a certain class in Turkey, a significant market has not yet emerged for smaller UAVs, and the majority of purchases are made from abroad. This situation is not strategically sustainable, especially for military UAV systems. Not only for military purposes but also for civil-purpose systems; The production of the gimbal and its electro-optic components in Turkey will provide economic and strategic benefits to our country.

In this project, the vibration isolation system and outer yoke of the gimbal system to be used for a small class UAV will be designed.

1.2 What are UAV and Gimbal?

Many different expressions are used for similar systems around the world, such as Drone, Unmanned Aerial Vehicles (UAV), Unmanned Aircraft Systems (UAS), and Remotely Controlled Aircraft Systems. Unmanned Aerial Vehicle-UAV instead of the term Drone has started used in the 1990s. In the 2010s, since the UAV only refers to the flying platform and needs at least a control station and a data link in addition to the platform for flight, the Unmanned Aircraft System (The term UAS) has started to become widespread. (Karaağaç,2016)

Although there is no common understanding after the general nomenclature is made, these aircraft are generally classified according to their various characteristics (weight, altitude, etc.). In this thesis, since the design of an electro-optical payload to be mounted on an unmanned aerial vehicle that will carry approximately 10 kg of payload and reach an

altitude of 2000 meters, this aircraft will be referred to as the "Mini UAV" in the thesis. We can define these mini unmanned air vehicles as UAVs with an average wingspan of 3-5 meters and a take-off weight between 5-40kg. An example mini-UAV suitable for the gimbal we will design in the thesis is shown in Figure 1.1.

In addition, throughout the thesis, the word gimbal, which normally means "A device for keeping an instrument such as a compass or chronometer horizontal in a moving vessel or aircraft, typically consisting of rings pivoted at right angles. ", will be used for the '2-axis Electro-Optical Surveillance System' being designed in this thesis.

Surveillance systems in UAVs are usually 2 or 3 axes. The meaning of a 2-axis gimbal is that the gimbal can rotate in 2 distinct axes. It contains different sensors and cameras used for different purposes. These are the day-TV camera for taking images during the day, the thermal camera for tracking hot objects, the laser pointer for the unmanned aerial vehicle to send the missiles to the target, and the GPS for determining the distance between the target and the gimbal. It is possible to have all of the units in the same system as well as merely one. It varies depending on the application sector and requirements. In addition, the motors, gears, belts, and bearings that provide the movement of these optical systems are located in these gimbals.

Figure 1.1 Example of Surveillance systems in UAV (www.controp.com)

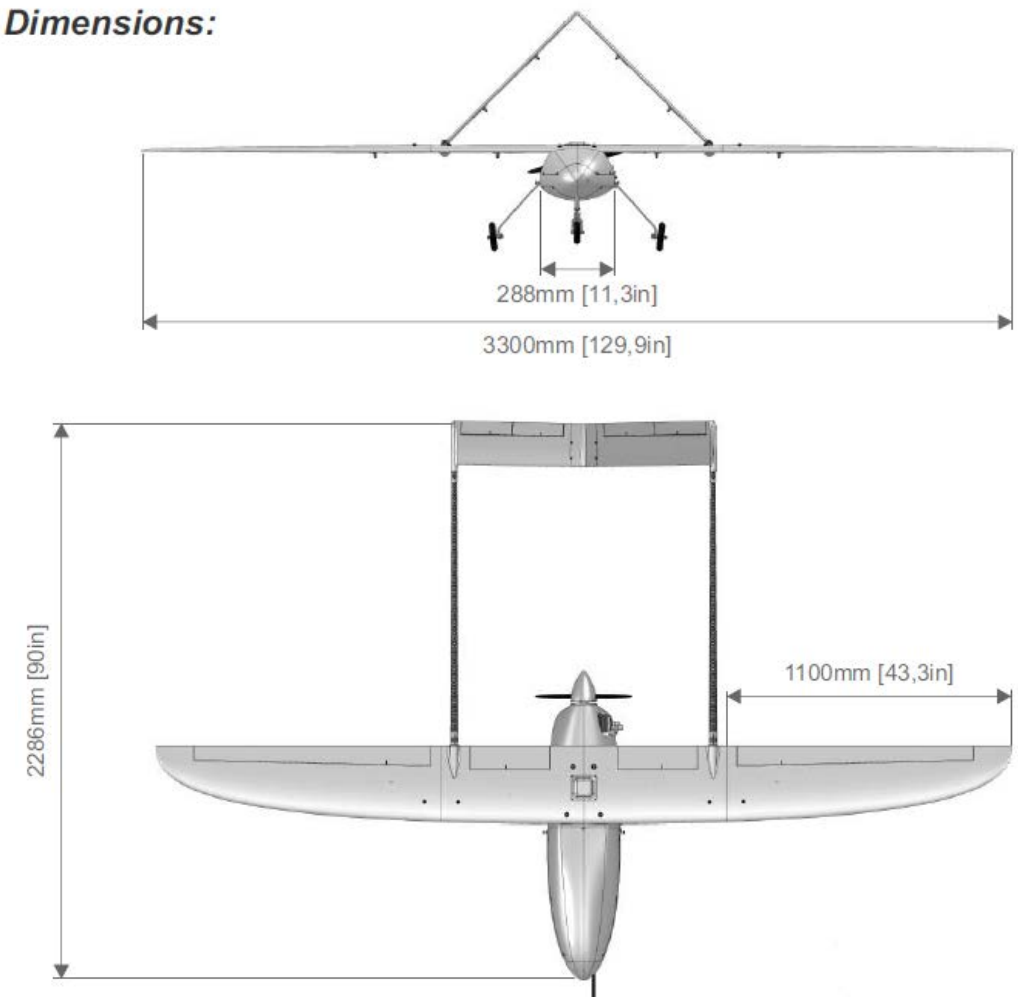

Figure 1.2 Example of Mini Class UAV (Dimensions of Penguin UAV) (uavfactory.com)

Figure 1.3 Example of Mini Class UAV (Stream C UAV) (Threod.com)

LITERATURE OVERVIEW

1.3 Patent Review for Vibration Isolation Systems of Gimbals

When "Gimbal", one of the keywords in our thesis topic, is searched on the site named Google Books Ngram Viewer, we see that this word has entered the books since the 1800s. Of course, this does not mean that the cameras have been stabilized with gimbals since the 1800s. Because one of the first places where the gimbal is used is the gyroscope that is used to detect the deviation of an object from its desired orientation. When looking at patents for the dates when imaging systems began to be stabilized using gimbals, the 1920s (United States, Patent No.US1634950, 1923) and 1930s (United States, Patent No. US1955770, 1933) are seen as early examples. If we examine the patent in 1927, its inventor describes: "Another object of the invention is to apply the said methods of stabilization to three specific instruments, which are used most commonly on balloons, airships and airplanes, namely observation instruments, bombsights, and aerial cameras. However, it is to be clearly understood that my novel methods of stabilization may be applied to any other instruments used on aerial craft or for any other purpose on air, sea, or land vehicles."

Since the 1960s, various patents have been obtained for products similar to today's gimbals, both in the field of active control (United States, Patent No. US11216013B2) and in the field of passive vibration isolation (United States, Patent No. US3638502) (United States, Patent No. US005184521A) (European patent, Patent No. P0559402A2, 1993) (World Intellectual Property Organisation, Patent No. WO1998016871A1, 1998) (United States, Patent No. US6263160, 2001).

As we approach today, we see a complex gimbal vibration isolator design in which coils spring, elastomer, and magnetic insulators are used together in a patent obtained in 2015 (World Intellectual Property Organisation, Patent No. WO9765925, 2015). Again in 2017 (United States, Patent No US2017175948A1, 2017), it is seen that coil springs, and elastomeric insulators are mentioned for a large and complex gimbal. In another patent related to the elastomer, a damper produced by molding rubber between metal plates used as a vibration isolator is mentioned. (United States, Patent No US10260591B2, 2019) Steel wire rope and viscous damper are also used as passive vibration isolators in UAVs, as seen in a sample patent (United States, Patent No US2020307826A1, 2020).

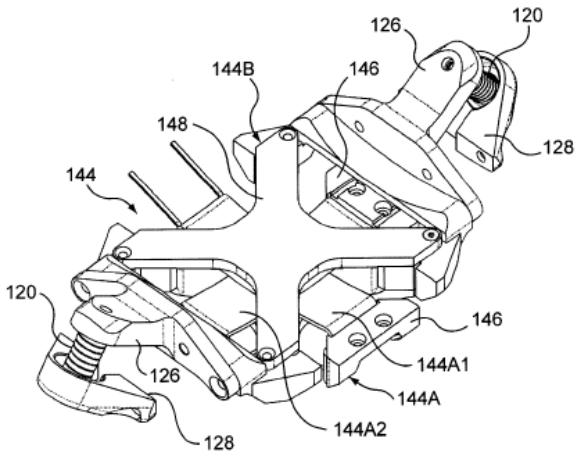

Figure 2.1 Vibration isolator design in which coils spring, elastomer and magnetic insulators. (World Intellectual Property Organisation, Patent No.WO9765925,2015)

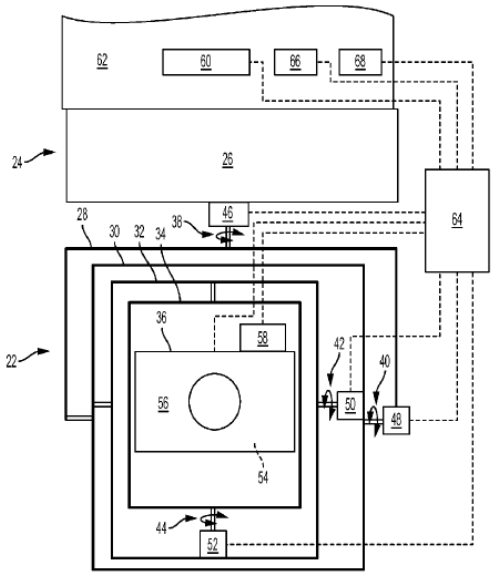

Figure 2.2 General parts of gimbal (United States, Patent No US2017175948A1,2017)

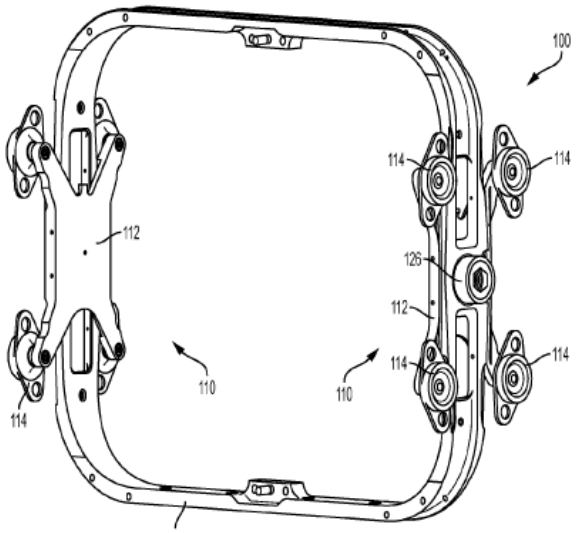

Figure 2.3 Inner yoke and elastomers (United States, Patent No US2017175948A1,2017)

1.4 Main Components of Gimbal

If we divide the gimbal into three basic parts as in shown Figure 2.5, the mount is the part that connects the gimbal and the UAV. Different mounts can be used on different air vehicle for the same gimbal, depending on the location of the connection points on the air vehicle. Optical ball is the part that contains the sensors, cameras, the motors that move the cameras and the brackets that hold these motors.

Within the scope of this thesis, the layout of the systems in the optical ball will not be examined, but the optical ball will be assumed as if black box whose center of gravity and geometric center coincide. To learn more information related to cameras can be reviewed the article named (Al Nuaimi, O.,2018).

Figure 2.4 Example cameras in the optic ball (flir.com)

Pan yoke contains motors for pan and tilt movement. Apart from this, depending on the design, bearings, vibration dampers, couplings, drive belts, and coolers, some electronic cards can be found in this part of the gimbal. In addition, there are nested frames inside the optic ball that keep the cameras parallel to the ground. These keep the camera stable with the gyroscope logic.

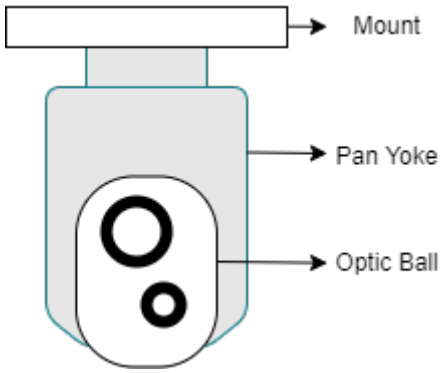

Figure 2.5 Main components of gimbal

1.5 Literature Review for Vibration Isolation Systems

Vibration, by its nature, is a problem that exists in many industries such as automotive, marine, and aerospace and needs to be solved. It is seen that basic solutions for vibration isolation can be used in different ways in different application areas, as well as in similar ways. For this, studies from different sectors that will provide a general understanding of vibration and various studies that directly deal with gimbal vibration have been researched and included in the literature survey.

Vibration isolation can generally be examined in two classes. These are active isolation and passive isolation. Active vibration isolation is the active application of force equal

and opposite to the forces exerted by external vibration. This system includes sensors that measure incoming vibration and actuators that produce motion that cancels this vibration.

Vibration isolation or reduction using rubber pads, steel wire, or mechanical springs is referred to as "passive vibration isolation.". The passive isolators exhibit some stiffness and damping, which are critical in constructing an effective isolator. The stiffness is used to calculate the isolator's corner frequency, which is often when the isolator begins to isolate vibration. When determining a system's absolute transmissibility, the corner frequency is important. For disturbances at frequencies above $\sqrt{2}\omega$, the absolute transmissibility is less than one, and vibration isolation occurs spontaneously. When the disturbance frequency is less than $\sqrt{2}\omega$, vibration amplification occurs. For disturbance frequencies much lower than the corner frequency, the absolute transmissibility is unity. Since the isolator performs best when the disturbance frequency is greater than $\sqrt{2}\omega$, The isolator's corner frequency should be kept as low as practicable. However, it is not possible to reduce the corner frequency too much for different reasons. One of these reasons is the spring deflection value. For example, when the system is under static loading, the isolator must both dampen vibration and support the static load. (Sciulli, D. ,1997)

When some damping methods that exist in the literature are investigated and the elements used in these designs are examined, products such as spring, damper, elastomer, ring, wire and, electromagnetic magnet are seen.

For example, in automotive, it is seen that the combination of spring coil and the viscous damper is used in the vehicle suspension system (Kumar, D. 2021) and the seat system (Tewari, V. K,1999) reduces the vibration reaching the driver. Elastomeric dampers are generally used to prevent the transmission of vibration generated by the internal combustion engine to the vehicle. (Bursa, Ali. İ. 2019)

Vibration isolation of large machines in buildings, such as air compressor units, is usually provided with coil springs to prevent damage to building integrity. (Nani, V. M.,2014)

(Ellison, J.,2001) conducts research on a circular steel ring in order to determine the effectiveness of a passive isolator in protecting avionics equipment from base excitation. SDOF is used to model the system. To begin, an experiment is carried out to acquire the ring's natural frequencies and modal damping, as well as to demonstrate that the

experimental results are consistent with the analytical results. After that, the acceleration response spectra of a concentrated mass attached to circular rings are examined. Finally, a correctly built circular ring is considered to provide effective protection of avionics equipment against any base excitation damages.

One of the methods used in vibration isolation is the material referred to as wire rope in the literature. (Balaji, P. S.,2017), (Weimin, C.,1997). A wire rope isolator is generally used for small action camera-like systems on the drone. In addition, it is seen that the cameras used in the cinema industry are also used in vibration isolation. When the patents are examined, it is seen that in the patent named (United States, Patent No US2020307826A1, 2020), the wire rope is used for vibration isolation of the camera attached to a rotary-wing UAV.

Apart from the aforementioned literature on vibration isolation, a literature search on gimbal design and analysis was also conducted. In the thesis titled '2 Axis Gimbal Camera Design' (Kuzey, N. B.,2007) both the mechanical design and electronic control of a 2-axis gimbal are mentioned. In this thesis, the mechanical design is not too complex and focused on the controller design since prototype production is also carried out.

The purpose of use of the gimbal is designed within the scope another thesis (Kerwin, J. M. J.,2018). Unlike ours, it is not aircraft but marine vehicles. However, it has been examined in this thesis considering that it will be useful in the design process. The scope of the thesis is a comprehensive example of an engineering designer's approach to solving a complex, open-ended design problem. Therefore, various design strategies are mentioned. In addition, it is thought to be a useful thesis on issues such as determining requirements and handling standards in the design process.

When examining an article (Mokbel, H. F.,2012). related to both vibration and gimbal design, it was seen that the natural frequencies of the parts were optimized using FEM modal analysis and also the weight was reduced.

When an article about Dynamics Modeling of the gimbal is examined, it is seen that the 7075-t3510 aluminum alloy used in aviation is used in the gimbal design. In addition, the structural analysis of the outer roll gimbal in the gimbal was analyzed; moreover, bending of the part mentioned as cantilever beam in the article under external force is analyzed. (Shen, C., 2020)

The article (Choi, J. W.,2021) in which not only the isolation system but also the modal analysis and harmonic response analysis of the entire gimbal assembly, was investigated. It was seen that this study aimed to examine the vibration characteristics for the development of a 2-axis stabilization gimbal for small UAVs and modal analysis and Harmonic response analysis were conducted to develop a 2-axis EO/IR yaw of less than 300 g.

WHAT IS THE VIBRATION AND ITS TYPES?

Vibration is a fluctuation of a mechanical or structural system about a datum position. The topic of vibration is related to the oscillatory motion of dynamic systems. The dynamic system consists of matter, which has mass and whose parts are capable of relative motion. The dynamic system consists of parts which has mass and whose parts are capable of relative motion. All of the bodies have mass and stiffness; due to the there is no infinite stiffness body, elasticity is able of vibration. Vibration can occur in many mechanical or structural systems. The vibration, which cannot be controlled, can cause to serious situations. Structural failure can happen due to large dynamic stresses, which can be caused by vibration. To minimize vibration, mathematical modelling of vibrations system is developed. The modelling provides to understanding of the principles governing the behaviour of vibrating systems and reducing the unwanted vibrations as little as possible. The basic mathematical model includes the mass, the spring, the damper and the excitation (Morse, 1963).

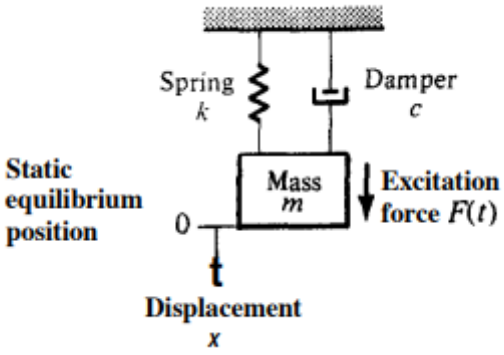

Figure 3.1 Basic mathematical model of vibratory system

The mass, m can be assumed as a rigid body. While the mass seen in Figure 3.1 vibrates, it can gain or lose kinetic energy depending on the change in velocity.

The spring, k has elasticity and negligible mass. If the spring can be deformed, the spring force can occur. The source of strain energy in the spring is the energy converted into spring potential energy by the work done. How much this potential energy change depends on the applied force and the amount of displacement. The spring rate is proportional to the measured in force per unit of deformation.

The damper, which is denoted by c, has no mass or elasticity. The energy applied to a damper are converted to heat. That is why, the damping element isn't conservative. Viscous damping, in which the damping force is proportional to the velocity, is called as linear damping. It is measured in force per unit velocity.

There are several types of vibration in a mechanic to understand their differences and difference in modelling; these are separated.

1.6 Free Vibration

Oscillations around a system's equilibrium position that occur without the application of an external excitation force are known as free vibration. Free vibration occurs when kinetic energy is applied to a system, resulting in a potential energy difference from the system's equilibrium position. (Kelly Graham, 2000)

To understand the model better, one-degree-of-freedom system is used.

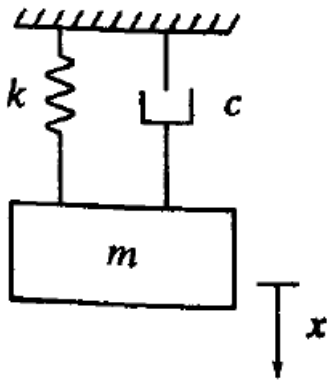

Figure 3.2 Mass- spring- damper system without excitation (Kelly Graham, 2000)

Newton's First Rule is applied on this system.

$$\sum F_{net} = ma \tag{3.1}$$

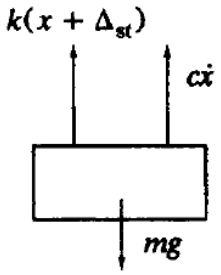

External forces

$$mg - k(x + \Delta_{st}) - c\dot{x} = m\ddot{x}$$

Analysis of the static equilibrium position reveals.

$$\Delta_{st} = \frac{mg}{k} \tag{3.2}$$

Finally, equations 3.1 & 3.2 to combined in one equation using some mathematical operations.

$$m\ddot{x} + c\dot{x} + kx = 0 \tag{3.3}$$

This equation is called as the differential equation of for free vibrations of a one-degree-of-freedom system.

1.6.1 Free Vibrations of Undamped One-Degree-of-System

The general form of the differential equation for undamped free vibrations of a one-degree-of-freedom is

$$m\ddot{x} + kx = 0 \tag{3.4}$$

Using initial conditions the equation of the free response can be solved.

$$x(0) = x_0$$

$$\dot{x}(0) = \dot{x_0}$$

$$x(t) = x_0 cos\omega_n t + \frac{\dot{x_0}}{\omega_n} sin\omega_n t$$

here;

$$\omega_n = \sqrt{\frac{k}{m}} \tag{3.5}$$

1.6.2 Free Vibrations of Damped One-Degree-of-System

The general form of the differential equation for damped free vibrations of a one-degree-of-freedom is

$$m\ddot{x} + c\dot{x} + kx = 0 \tag{3.6}$$

This equation can be divided into m.

$$\ddot{x} + \frac{c}{m}\dot{x} + \frac{k}{m}x = 0$$

Critical damping coefficient is defined as : $c_c = 2\sqrt{km}$

After that, the damping ratio also defined as $\zeta = \frac{c}{c_c} = \frac{c}{2\sqrt{km}}$

Then this equation can be written as :

$$\ddot{x} + 2\zeta\omega_n \dot{x} + {\omega_n}^2 x = 0 \tag{3.7}$$

It is the standard form of the differential equation governing the free- vibrations of a one-degree-of -freedom system with viscous damping.

The damping ratio (ζ) that can vary from undamped ($\zeta = 0$), underdamped ($\zeta < 1$) through critically damped ($\zeta = 1$) to overdamped ($\zeta > 1$). These three cases should be examined to explore the behaviour of the system's response.

Cases 1: $\zeta < 1$ (Underdamped Free Vibrations)

Due to $\zeta < 1$, the roots of exist as a complex conjugate pair.

$$r_{1,2} = \omega_n(-\zeta \pm \mathrm{i}\sqrt{1-\zeta^2}\,)$$

Then, general response equation becomes :

$$x(t) = e^{-\zeta\omega_n t}(C_1\cos(\omega_n(\sqrt{1-\zeta^2}\,t) + C_2\sin(\omega_n\left(\sqrt{1-\zeta^2}\,t\right)\right)$$

Applying initial conditions to this equation, it becomes :

$$x(t) = e^{-\zeta\omega_n t}(\cos(x_0\omega_n(\sqrt{1-\zeta^2}\,t) + \frac{\dot{x_0} + \zeta\omega_n x_0}{\omega_n\sqrt{1-\zeta^2}}\sin(\omega_n\left(\sqrt{1-\zeta^2}\,t\right)\right)$$

Cases 2 : ζ = 1 (Underdamped Free Vibrations)

For ζ = 1 , there is only one real root

$$r_{1,2} = -\omega_n$$

Then, general response equation becomes :

$$x(t) = e^{-\zeta\omega_n t}(C_1 + C_2 t)$$

Applying initial conditions on this equation, it becomes :

$$x(t) = e^{-\zeta\omega_n t}(x_0 + (\dot{x_0} + \omega_n x_0)t)$$

Cases 3 : ζ >1 (Overdamped Free Vibrations)

For ζ = 1 , there are two real, distinct roots

$$r_{1,2} = \omega_n(-\zeta \pm \sqrt{\zeta^2 - 1}\,)$$

Then, general response equation becomes with applying boundary conditions :

$$x(t) = \frac{e^{-\zeta\omega_n t}}{2\sqrt{\zeta^2-1}}\left\{\left[\frac{\dot{x_0}}{\omega_n} + x_0(\zeta + \sqrt{\zeta^2 - 1}\,)\right] e^{\omega_n\sqrt{\zeta^2-1}\ t} + \left[-\frac{\dot{x_0}}{\omega_n} + x_0(-\zeta + \sqrt{\zeta^2 - 1}\,)\right] e^{-\omega_n\sqrt{\zeta^2-1}\ t}\right\}$$

Finally, these three displacement graphs can be plotted versus time.

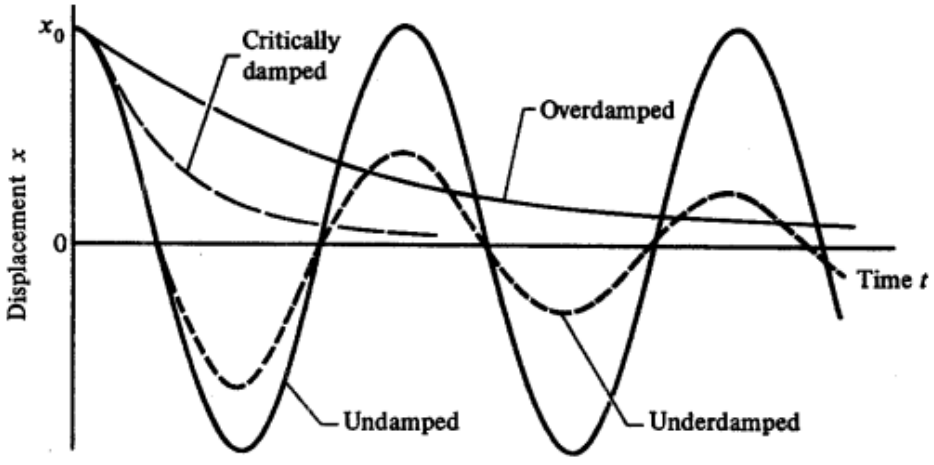

Figure 3.3 Free vibrations of the systems

1.7 Forced Vibration

The motion of a system that occurs in response to a continuous excitation whose magnitude fluctuates sinusoidally with respect to time is called forced vibration. The excitation can be caused by the force applied to the system or by the movement of the foundation supporting it.

1. The External Forcing model is a behaviour of the system which has a time-varying force acting on it.
2. Base Excitation model is the behaviour of the vibration isolation system. The base of the spring can be given the prescribed motion that causing the mass to vibrate. This system is also termed motion transmissibility for the system. (Harris,2002)

Forced vibration is oscillations about a system's equilibrium position that occur in with external excitation force.

$$m\ddot{x} + c\dot{x} + kx = F_{eq}(t) \tag{3.8}$$

where

$$F_{eq}(t) = F_O \sin(\omega t + \varphi)$$

This equation can be written as :

$$\ddot{x} + 2\zeta\omega_n \dot{x} + {\omega_n}^2 x = \frac{F_0}{m_{eq}} \sin(\omega t + \varphi)$$

The right side is not equal to zero. Thus, we have also partial solution for the response equation.

$$x(t) = x_h(t) + x_p(t) \tag{3.9}$$

The homogenous solution is solved as a free vibration response. To solve the partial solution , some differential-algebraic manipulations are used

$$x_p(t) = A \sin(\omega t + \varphi) + B \cos(\omega t + \varphi)$$

$$\dot{x_p}(t) = A\omega \cos(\omega t + \varphi) - B\omega \sin(\omega t + \varphi)$$

$$\ddot{x_p} = -A\omega^2 \sin(\omega t + \varphi) - B\omega^2 \cos(\omega t + \varphi)$$

These equations can be put inside the differential equation, and partial solution can be found.

The particular solution of the standard form of the differential equation governing the motion of a viscously damped single-of-freedom system with force excitation can be found as :

$$x_p(t) = \frac{F_0}{m_{eq}[(\omega_n^2 - \omega^2)^2 + (2\zeta\omega_n\omega)^2]} [-2\zeta\omega_n\omega \cos(\omega t + \varphi) + (\omega_n^2 - \omega^2)\sin(\omega t + \varphi)]$$

After some algebraic manipulations, the equation can have a new form :

$$x_p = X \sin(\omega t + \varphi - \emptyset)$$

$$X = \frac{F_0}{m_{eq}[(\omega_n^2 - \omega^2)^2 + (2\zeta\omega_n\omega)^2]^{1/2}}$$

$$\emptyset = tan^{-1}(\frac{2\zeta\omega_n\omega}{\omega_n^2 - \omega^2})$$

where X is the amplitude of the forced response and $\emptyset$ is the phase angle between response and the excitation. These equation can be converted to nondimensional forms to understand well.

$$X = f\ (F_0\ , m_{eq}, \omega\ , \omega_n\ , \zeta\ )$$

$$\emptyset = g(\omega\ , \omega_n, \zeta)$$

The above equation when multiplied with $\frac{m_{eq}\omega_n^2}{F_0}$

$$\frac{m_{eq}\omega_n^2 X}{F_0} = \frac{1}{[(1 - r^2)^2 + (2\zeta\ r)^2]^{1/2}}$$

where $r = \frac{\omega}{\omega_n}$ is a frequency ratio. The ratio becomes

$$M = \frac{m_{eq}\omega_n^2 X}{F_0}$$

M is the and is often called the magnification factor, which provides to interpretation is that of the maximum force developed in the spring mass- damper system to the maximum value of the exciting force. Thus the nondimensional form becomes :

$$M(r,\zeta) = \frac{1}{\sqrt{(1-r^2)^2+(2\zeta r)^2}} \tag{3.10}$$

The magnification factor becomes the function of the frequency ratio for different values of ζ damping ratio.

- when r = 0 , M = 1 . The maximum force created in the spring-mass-damper system is equal to the value of the exciting force in this situation since the excitation force is constant.
- When r goes to the infinity, M goes to the zero, which means that amplitude of the forced response is very small for high frequency excitations.
- The magnification factor grows without bound only for ζ =0. For $0 < \zeta \leq 1/\sqrt{2}$, the magnification factor has a maximum for some value of ζ.
- For $\zeta > 1/\sqrt{2}$, M monotonically decreases with increasing r.

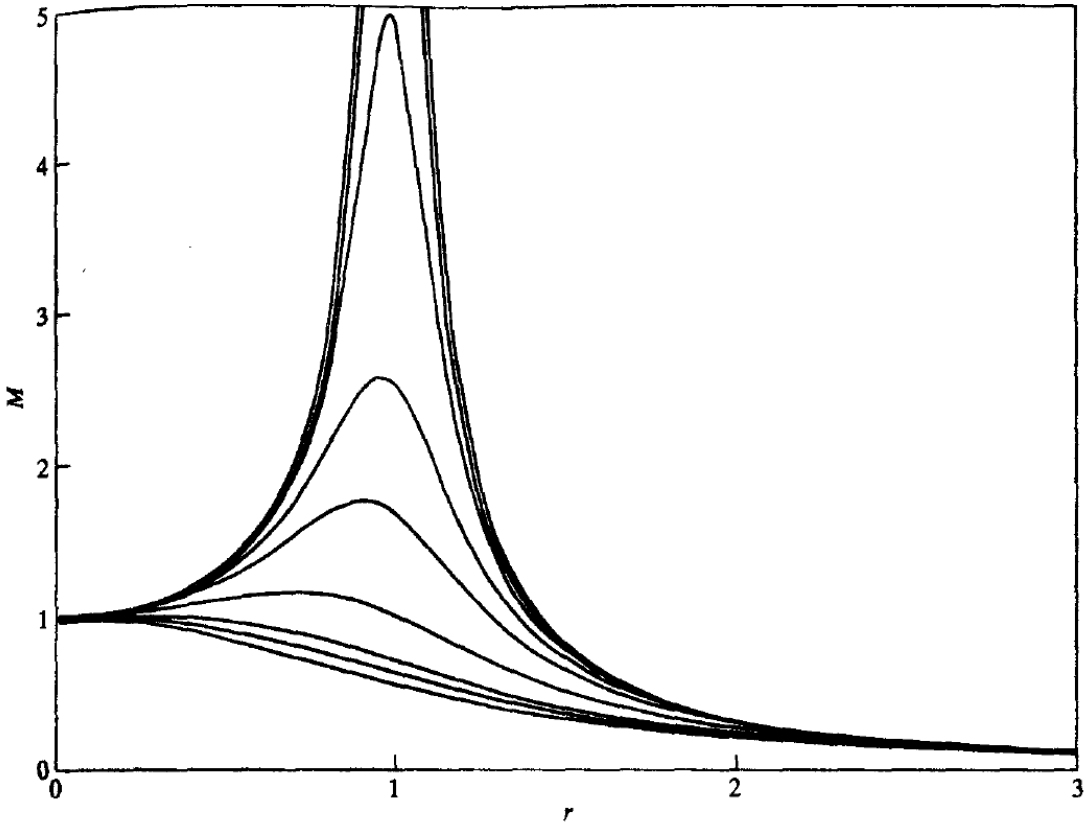

Figure 3.4 Magnification factor versus frequency ratio for different damping ratios

From Figure 3.4, it is very clear that the magnification factor becomes maximum when r = 1, which means that the frequency of the system is equal to the natural frequency. This situation is called as resonance. Resonance can be described as the increasing amplitude that occurs when the frequency of the applied periodic force is equal or very close to the natural frequency of the system on which it acts. When an excitation force can be applied at a resonant frequency of the dynamic system, the system can oscillate at a higher amplitude than when the same force can be applied at other, non-resonant frequencies.

MECHANICAL COMPONENTS OF VIBRATION ISOLATOR SYSTEM

1.8 Springs

Spring is a mechanical device that provides to store mechanical energy and exerts forces or torques. Spring can also be expressed as any machine or component which deforms under applied force and comes to the back position when force is removed acts. Generally, spring is a nonlinear element ,but it behaves linearly in a smaller range working range δ. Springs are generally made out of metal (annealed steel hardened after fabrication, plain carbon steels, alloy steels, corrosion-resisting steels and etc.) and, for small loads or minimum mass by plastics or composite materials Depending on the needs, almost any material with the right combination of flexibility and stiffness can be used to create the mechanical spring. A spring rate (stiffness, which is denoted by k) can be defined as the change in the force divided by the change in the spring deflection (δ).

1.8.1 Types of Springs

Springs can be classified depending on their construction and line of action of applied force. According to this classification method, there are following types of spring is listed below.

1. Helical Spring
    - Tension/extension springs
    - Compression springs
    - Torsion spring
2. Leaf Spring
3. Disc Spring
    - Belleville
    - Slotted Disc
    - Contact Disc
    - Curved Disc
    - Wave Spring
    - Finger Washer

1.8.1.1 Helical or Coil Spring

A helical spring is also known as a coil spring. They can be made of wire coiled in the form of a helix. The cross-sectional area of the coil wire can be produced in different ways according to its purpose. For example, it can be round, rectangular, or square.

This spring can be divided to three main categories depending on its load.

- Tension/extension springs – This type of springs can be designed to operate with a tension load. As a result of the applied force, the spring stretches and elongates.
- Compression springs – This type of springs can be designed to operate with a compression load. As a result of the applied force the spring becomes shorter.
- Torsion spring – Unlike tension and compression springs, which are loaded with an axial force, torsion springs are loaded with a torque or twisting force, which causes the end of the spring to spin through an angle when the force is applied.

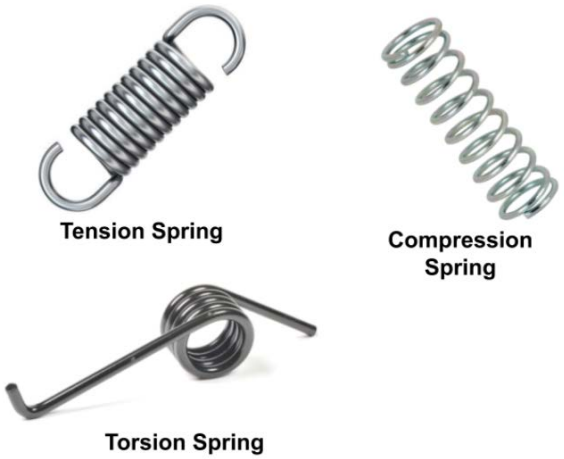

Figure 4.1 Types of helical springs depending on the load (spring smlease.com)

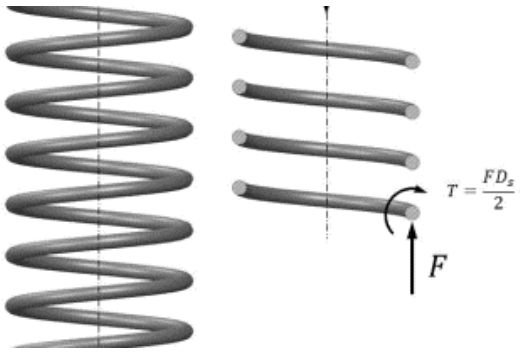

Figure 4.2 Axially loaded helical spring and free body diagram (Min-Chie,2015)

Figure 4.2 (Min-Chie, C. H. I. U,2015) illustrates the round-wire helical compression spring-loaded by the axial force F. D denotes the mean coil diameter and d as the wire diameter. The next figure is a portion of it removed, and the effect of the removed portion can be replaced by the net internal reactions. Then, as shown in the figure, from equilibrium, the cut section would contain a direct shear force F and a torsion T = F*D/2.

To calculate shear stress, spring index (C), which means that a measure of coil curvature can be used in the shear stress equation using mean coil diameter and wire diameter.

$$C = \frac{D}{d} \tag{4.11}$$

Spring index (C) varies between 4 to 12.

Shear stress equation becomes

$$\tau = K_s \frac{8FD}{\pi d^3} \tag{4.12}$$

K_s is the shear-stress correction factor. Its formula is $K_s = \frac{2C+1}{2C}$

Generally, K_s is replaced by another K factor, which corrects for both curvature and direct shear.

$$K_B = \frac{4C+2}{4C-3} \tag{4.13}$$

K_B is the Bergstrasser factor.

Finally, the maximum shear stress can be calculated as:

$$\tau = K_B \frac{8FD}{\pi d^3} \tag{4.14}$$

To find spring rate (k) for helical springs, strain energy, and Castigliano's theorem can be used. Then, the equation becomes:

$$k = \frac{F}{\delta} = \frac{d^4 G}{8D^3 N_a} \tag{4.15}$$

where ;

G: shear modulus

N_a : number of active coils

1.8.1.2 Compression Spring

When a compression force is applied to the compression springs, their length reduces. They operate in compression load.

There are four types of ends for compression springs. These are plain end, plain and ground, squared and squared and ground.

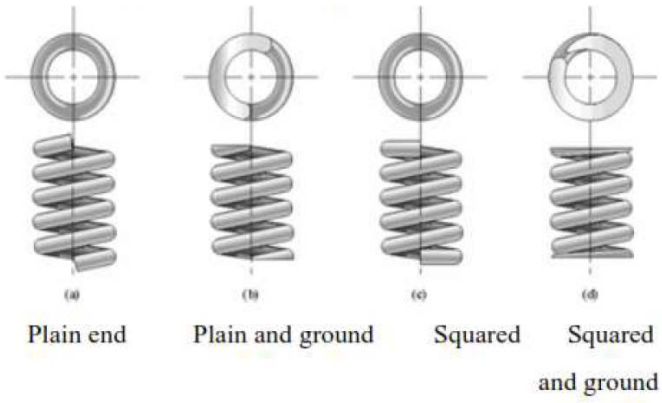

Figure 4.3 Types of ends for compression spring

According to their types of spring ends, formulas for the dimensional characteristics of compression spring can change.

Table 4.1 Compression spring formulas for dimensional characteristics

Types of Spring Ends				
Term	Plain	Plain and Ground	Squared or Closed	Squared and Ground
End coils, N_e	0	1	2	2
Total coils, N_t	N_a	$N_a + 1$	$N_a + 2$	$N_a + 2$
Free length, L_0	$pN_a + d$	$p(N_a + 1)$	$pN_a + 3d$	$pN_a + 2d$
Solid length, L_s	$d(N_t + 1)$	dN_t	$d(N_t + 1)$	dN_t
Pitch, p	$(L_0 - d)/N_a$	$L_0/(N_a + 1)$	$(L_0 - 3d)/N_a$	$(L_0 - 2d)/N_a$

Spring Material

Springs are manufactured hot or cold working processes depending on the size of material, spring index, and properties of desired.

The ultimate tensile stress of spring varies with a diameter as

$$S_{ut} = \frac{A}{d^m}$$ A, m and given in Figure 4.4 (Carlson, H.,1978).

Material	ASTM No.	Exponent *m*	Diameter, in	*A*, Kpsi.in^m	Diameter, mm	*A*, MPa.mm^m	Relative Cost of Wire
Music wire*	A228	0.145	0.004–0.256	201	0.10–6.5	2211	2.6
OQ&T wire†	A229	0.187	0.020–0.500	147	0.5–12.7	1855	1.3
Hard-drawn wire‡	A227	0.190	0.028–0.500	140	0.7–12.7	1783	1.0
Chrome-vanadium wire§	A232	0.168	0.032–0.437	169	0.8–11.1	2005	3.1
Chrome-silicon wire‖	A401	0.108	0.063–0.375	202	1.6–9.5	1974	4.0
302 Stainless wire#	A313	0.146	0.013–0.10	169	0.3–2.5	1867	7.6–11
		0.263	0.10–0.20	128	2.5–5	2065	
		0.478	0.20–0.40	90	5–10	2911	
Phosphor-bronze wire**	B159	0	0.004–0.022	145	0.1–0.6	1000	8.0
		0.028	0.022–0.075	121	0.6–2	913	
		0.064	0.075–0.30	110	2–7.5	932	

Figure 4.4 Constants A and m of Sut = A/d^m for estimating minimum tensile strength of common spring wires

Then mechanical properties of some spring wires is listed below .

Material	Elastic Limit, Percent of S_{ut}		Diameter *d*, in	*E*		*G*	
	Tension	Torsion		Mpsi	GPa	Mpsi	GPa
Music wire A228	65–75	45–60	<0.032	29.5	203.4	12.0	82.7
			0.033–0.063	29.0	200	11.85	81.7
			0.064–0.125	28.5	196.5	11.75	81.0
			>0.125	28.0	193	11.6	80.0
HD spring A227	60–70	45–55	<0.032	28.8	198.6	11.7	80.7
			0.033–0.063	28.7	197.9	11.6	80.0
			0.064–0.125	28.6	197.2	11.5	79.3
			>0.125	28.5	196.5	11.4	78.6
Oil tempered A239	85–90	45–50		28.5	196.5	11.2	77.2
Valve spring A230	85–90	50–60		29.5	203.4	11.2	77.2
Chrome-vanadium A231	88–93	65–75		29.5	203.4	11.2	77.2
A232	88–93			29.5	203.4	11.2	77.2
Chrome-silicon A401	85–93	65–75		29.5	203.4	11.2	77.2
Stainless steel							
A313*	65–75	45–55		28	193	10	69.0
17-7PH	75–80	55–60		29.5	208.4	11	75.8
414	65–70	42–55		29	200	11.2	77.2
420	65–75	45–55		29	200	11.2	77.2
431	72–76	50–55		30	206	11.5	79.3
Phosphor-bronze B159	75–80	45–50		15	103.4	6	41.4
Beryllium-copper B197	70	50		17	117.2	6.5	44.8
	75	50–55		19	131	7.3	50.3
Inconel alloy X-750	65–70	40–45		31	213.7	11.2	77.2

Figure 4.5 Mechanical properties of some spring wires

1.8.1.3 Tension Spring

Tension coil types of springs operate in tension loads. In the tension springs, springs coils are spaced at a short distance.

1.8.1.4 Torsion Spring

Torsion types of springs store twisting force.

1.8.1.5 Leaf Spring

Leaf spring consists of several flat plates of different lengths. These plates are sandwiched one on another using clamps and bolts. These are also known as carriage or semi-elliptical springs. They play the role of key elements in the suspension systems of automotive vehicles such as trucks, heavyweight vehicles, railroad vehicles and etc.

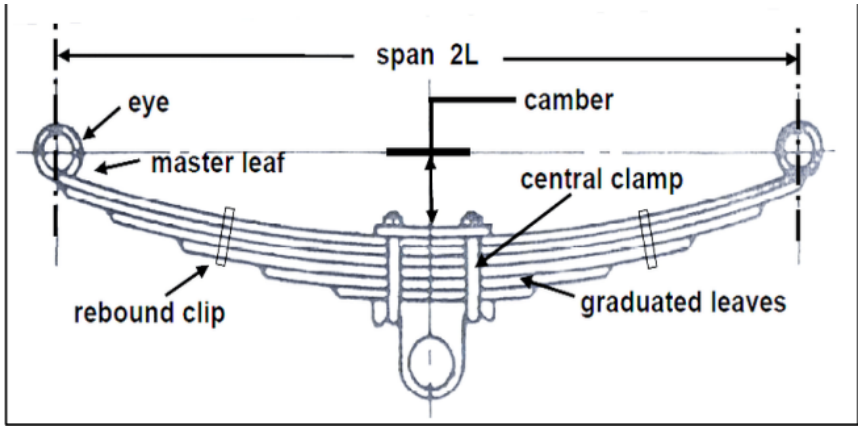

Figure 4.6 Leaf spring model (Kushwah, S., 2020)

1.8.1.6 Disc Spring

The disk spring is the round-shaped conical disk that can deform at a relatively shorter distance when compressive force is applied at the disk axis.

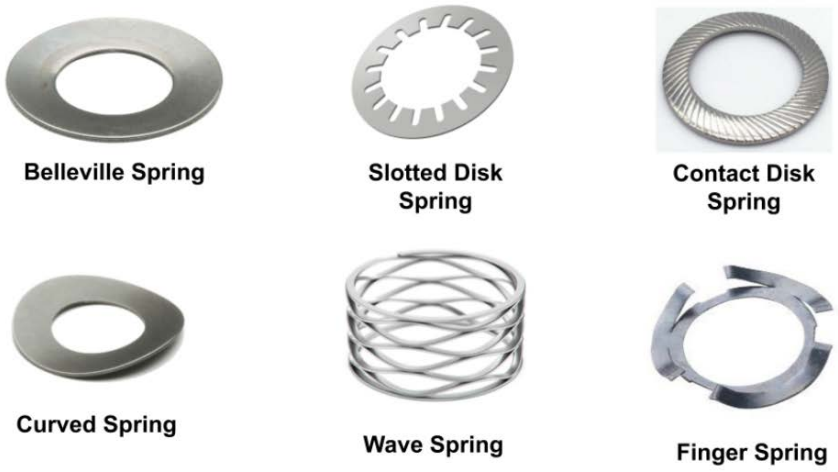

Figure 4.7 Types of some disc (spring smlease.com)

1.9 Springs in Combination

Springs can be placed in the combination. It is suitable for purposes of modelling and analysis to replace the combination of springs with a single spring of an equivalent spring stiffness, k_{eq}. The equivalent stiffness can be determined such that the system with a combination of springs has the identical displacement, x, as the equivalent system when both systems are subjected to the identical force, F. A model one- degree-of-freedom system consisting of a block hooked up to the spring of an equivalent stiffness can be shown in the figure.

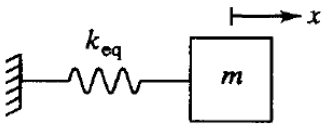

The resultant force acting on the block will be written as :

$$F = k_{eq}\, x \tag{4.16}$$

When the springs in the system are parallel, the displacement of each spring in the system is the same. However, the resultant force acting on the block becomes the sum of the forces developed in parallel springs. If x is displacement of the block, then force develop in the i^{th} spring is k_i x and the resultant is:

$$F = k_1\, x \; + \; k_2\, x + \cdots \; k_n\, x = \left(\sum_{i=1}^{n} k_i\right) \text{x} \tag{4.17}$$

Using these equations, k_{eq} can be written as :

$$k_{eq} = \sum_{i=1}^{n} k_i \tag{4.18}$$

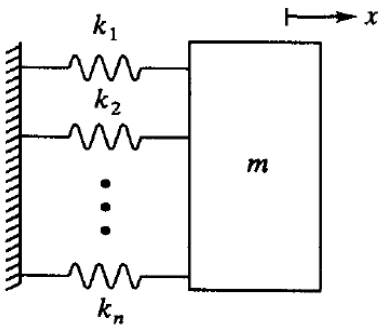

The springs are serial in the figure. The force developed in each spring is the same and equal to the force acting on the block. The displacement of the block becomes the sum of the changes in the length of the springs in the series combination. If x_i is the change in length of the i^{th} spring, then

$$x = x_1 + x_2 + \cdots x_n = \sum_{i=1}^{n} x_i$$

Since the force is the same in each spring $x_i = F/ k_i$ and equation becomes

$$x = \sum_{i=1}^{n} \frac{F}{k_i} \tag{4.19}$$

Since the series combination can be replaced by a spring of an equivalent stiffness can be calculated as :

$$k_{eq} = \frac{1}{\sum_{i=1}^{n} k_i} \tag{4.20}$$

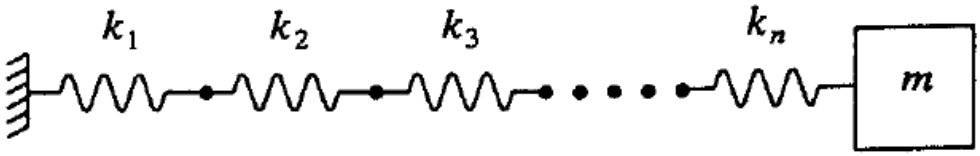

1.10 Dampers

In physics, damping is the process of dissipating energy to prevent vibratory motion such as mechanical oscillations, noise, and alternating electric currents. Automobile shock absorbers, aviation isolators, and vibration pad for air compressors are examples of dampening devices. (Britannica, T. ,2020)

If there is no damping and the system is forced to vibrate, the response or amplitude of the vibration tends to increase near resonance. Vibration amplitude is always limited by dampening. It may be able to avoid resonance by altering the system's natural frequency if the excitation frequency is known. A variable-speed electric motor or an internal combustion engine, for example, may need the system or machine to run at a variety of speeds. Under all operational conditions, it could be impossible to avoid resonance. In such instances, we can employ structural materials with high internal damping to add damping into the system and manage its reaction. (Singiresu, S. R.,1995)

There are different types of dumping models and materials whose working principles are based on these models. The two most popular of these are viscose, Coulomb, or dry-friction damping, and viscous damping. By simply explaining the coulomb methods, the damper systems working with the viscous damping method, which we will use in the scope of the thesis, will be discussed in more detail.

Coulomb damping is a sort of continuous mechanical damping in which sliding friction absorbs the kinetic energy of the system. Friction occurs when two solid bodies slide on one other. When a single-degree-of-freedom system that has Coulomb or dry-friction damping, is exposed to a harmonic force $F(t) = F_0 sin\omega t$, the equation of motion is given by

$$m\ddot{x} + kx \pm \mu N = F(t) \tag{4.21}$$

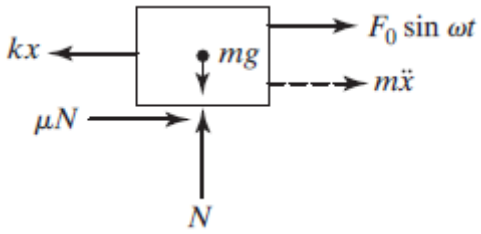

Since viscous damping is expressed by linear equations of motion, it is a common and simple damping method in practice. A viscous fluid damper is generally made out of a piston within a damper housing filled with silicone or a similar oil. Fluid orificing allows energy to be dispersed by passing the fluid through multiple tiny orifices from one side of the piston to the other. Viscous damping contains taking advantage of the high flow resistance of viscous fluids. The forces that occurred in the viscous damper are

proportional to the velocity of its deformation. Fluid viscous dampers put out virtually zero force at the low velocities related to thermal motion. The fluid viscous damping device called dashpot is shown in Figure 4.8 (Warnotte, V., 2007).

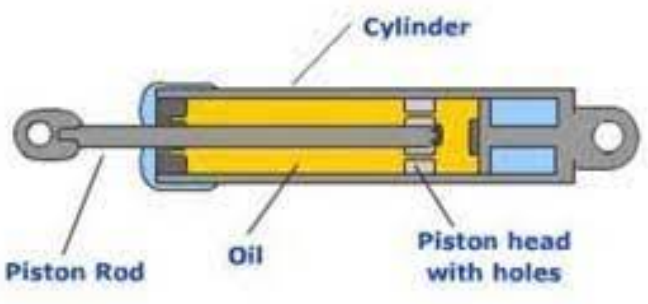

Figure 4.8 Dashpot and its components (Warnotte, V., 2007)

Viscous damping force F is proportional to the velocity $\dot{x}$ or v and is expressed as below.

$$F = -c\dot{x}$$

where c is the damping constant or coefficient of viscous damping, and the negative sign shows that the damping force is opposite to the direction of velocity and its unit is mass per time. Viscous damping causes to exponential decay in amplitude of free vibrations, and a reduction in the amplitude in forced vibration can be caused by harmonic excitation.

The dashpot's upper plate should be linked to a sturdy body. The plate glides across a reservoir of viscous liquid with dynamic viscosity as the body moves. A is the area of the plate that comes into contact with the liquid. Shear stress between the fluid and the plate might develop, resulting in a friction force acting on the plate. Assume the reservoir is fixed and the top plate moves at v over the liquid. Because the reservoir depth h is shallow enough, the liquid velocity profile becomes almost linear.

$$u(y) = v\frac{y}{h}$$

The shear stress that occurred on the plate is determined by Newton's viscosity law

$$\tau = \mu\frac{du}{dy} = \mu\frac{v}{h}$$

The viscous force acting on the plate is

$$F = \tau A = \frac{\mu A v}{h}$$

$$F = -c\dot{x}$$

$$c = \frac{\mu A}{h} \tag{4.22}$$

1.11 Elastomers

Pneumatic, hydraulic, elastic metal, and elastomeric designs can be commonly used in commercial vibration isolation applications. More preferred among these are generally elastomers, and they are commonly used in the industry. Usually used design consisting of elastomeric material bonded to metal plates or a metal core. Such isolators can be typically called elastomeric mounts. There are various elastomer types that are used in this type of mount and some examples of their materials are natural rubber, neoprene, and butyl rubber. (Sudhir Kaul,2021)

The reason elastomers are so common is being able to work at high stresses without breaking and, in some ways high load-carrying capacity. However, the standard model mentioned in chapter 3 consists of a linear spring of stiffness k and viscous damper with damping coefficient c. In this simple model, k and c are constants independent of frequency. Although this approach that illustrates the basic principles of vibration isolation, it is not amenable to the analysis of elastomers where both k and c vary with frequency. Thus, C_c, and f_n, will depend on frequency and iterative calculations.

For elastomeric components, the degree of isolation and damping achieved will depend not only on the dynamic properties but also on the static properties since in many cases, the component is also required to carry a static load. Thus, in assessing mount performance, it is necessary to consider both the static and dynamic properties of the elastomer and the geometry of the design.

Table 4.2 Some Necessary Requirements for Elastomer Design

Basic Design Requirements for Elastomers	
Specifications for the equipment to be isolated	weight, size, center of gravity, and inertias
Types of dynamic disturbance to be isolated	sinusoidal and random vibration, frequency and magnitude of inputs,
Ambient environmental conditions	temperature ranges, humidity, ozone, exposure to oils
Allowable system responses	what is the maximum system deflection allowed

In most applications, the performance of the product is determined by the elastomer modulus and by details of the product's geometry. Also, there are many factors that change the elastomer modulus, such as frequency, temperature, and static loading. However, some fundamental equations will outline static stress-strain relationships in bonded rubber components of various geometrical configurations.

$$k_s = \frac{AG}{t} \qquad (shear\ spring\ rate)$$

$$k_c = \frac{AE_c}{t} \qquad (compression\ spring\ rate)$$

$$k_t = \frac{AE_t}{t} \qquad (tension\ spring\ rate)$$

A is effective load area (m^2)

t is the thickness (m) of the undeformed elastomer

G, E_c, and E_t represent the shear, compression, and tension modulus (KPa) of the elastomer.

$$shape\ factor\ S = \frac{load\ area}{bulge\ area}$$

$$for\ example\ shape\ factor\ for\ the\ rectangular\ block = \frac{(length)(width)}{2t(length + width)}$$

$$E_c = 1.33 * E_0(1 + \emptyset S^2)$$

$$E_0 = Young's\ modulus$$

$$\emptyset = elastomer\ compression\ coefficient$$

METHODS

1.12 What are FFT and PSD?

In order to determine whether a mechanical component will be damaged by vibration, first of all, the characteristics of the vibration to which the part is exposed, such as frequency and amplitude, must be known.

Vibration data can be obtained either from guidelines prepared for vibrations under various conditions (MIL-STD-810) or from vibration sensors. Vibration analysis begins by plotting amplitude versus time. This is called time-domain data. These data are obtained from the various sensors. Usually, such data do not yield meaningful results, and it is necessary to convert them to the frequency domain.

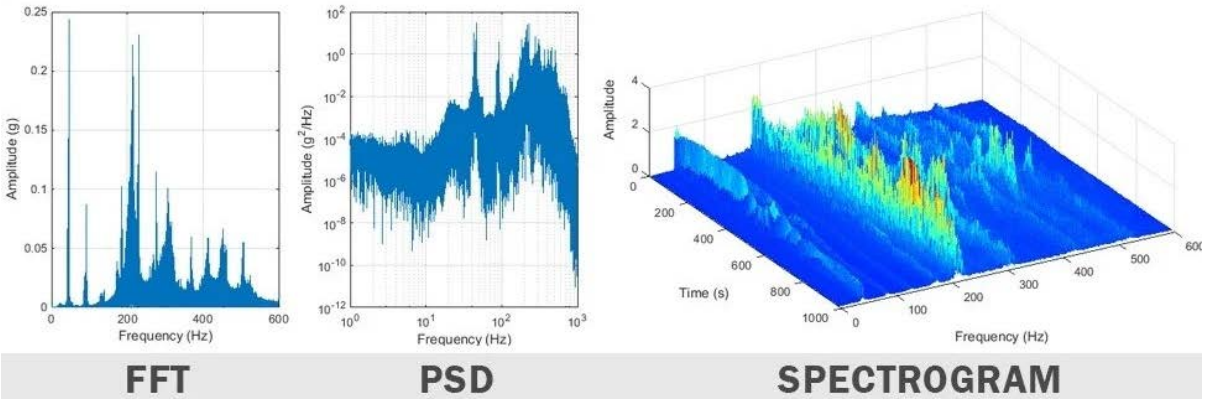

Figure 5.1 Different methods can be used to convert data in the time domain to frequency domain. (blog.endaq.com)

"Fast Fourier Transform" (FFT) converts a signal into individual spectral components and thereby contributes frequency information about the signal. FFT is the optimized algorithm for applying the "Discrete Fourier Transform" (DFT). The signal can be sampled over a period of time and divided into frequency components. These components are single sinusoidal oscillations of different frequencies, each with its own amplitude and phase. This transformation can be illustrated in the diagram below. During the measured time period, the signal contains three distinct dominant frequencies. (Wang, Y.,2020).

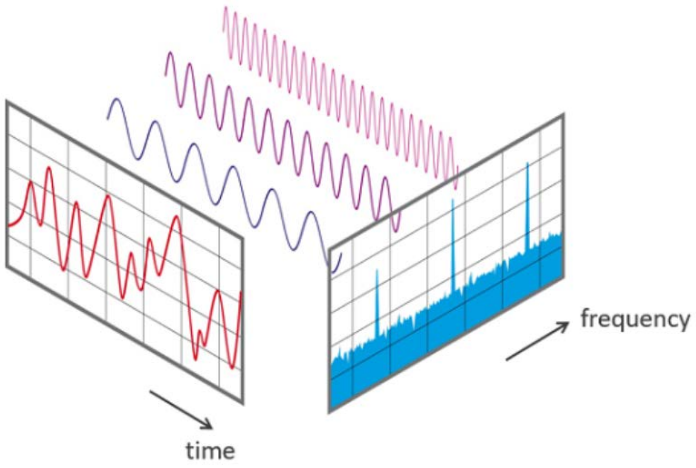

Figure 5.2 FFT Analysis frequency and time domain graphs (blog.endaq.com)

As shown in Figure 5.2, FFT is a useful method for detecting the frequencies of several overlapping sine waves, but in the real world, there are many more overlapping frequencies. This large number of overlapping frequencies can be expressed as random vibrations.

Since it would be difficult to specify random vibration in terms of several frequencies, the method called Power Spectrum Density is used to specify the characteristics of random vibration. In the graphs obtained by this method, the horizontal axis is the frequency axis and goes from zero to a certain value. The vertical axis represents the amplitude. Thus, the amplitude of the vibration at each frequency value is known in terms of the square of the acceleration (g^2). The graphs in which the frequency and amplitude information is added to the time information are called 'spectrogram'. These three different analyzes and their graphs are shown in Figure 5.1.

In order to graph these data, it is necessary to make measurements with experimental methods. However, some standards offer ready-made vibration charts of some commonly used vehicles (airplane, helicopter, truck). One of the most widely used guidelines, MIL-STD-810, is a set of performance and manufacturing guidelines adjusted by the US Department of Defense for military and commercial equipment and applications. These guidelines specify the allowable ranges of parts and environmental conditions a device must operate to ensure compatibility. The vibration part occupies an important place in this document. The vibrations that various equipments are exposed to while being

manufactured, transported or in operation have been made into PSD graphics by making a generalization.

In this thesis, if the mini-UAV is considered a propeller aircraft exposed to vibration during flight, the PSD graph in Figure 5.3 can be used as vibration data in the analysis. However, since the dimensions and materials of the aircraft mentioned in this guide are different from our UAV, this graphic was not taken as a reference within the scope of the thesis.

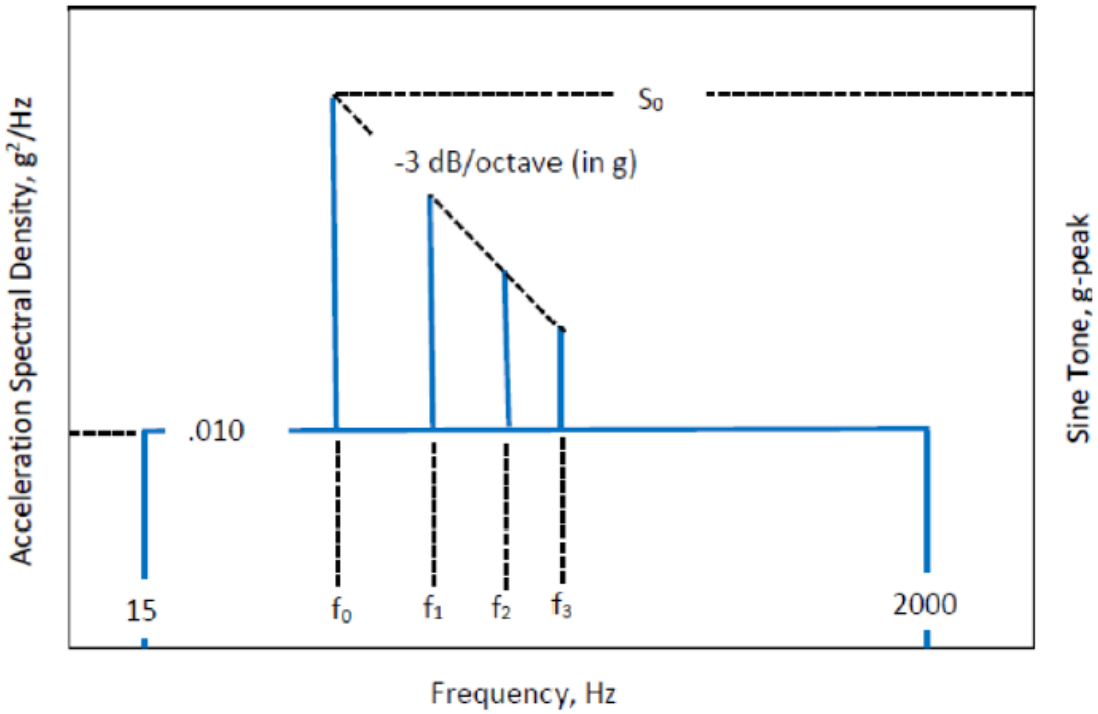

Figure 5.3 PSD Graph for propeller aircraft ("Download MIL-STD-810H")

1.13 Topology Optimization

1.13.1 What is the topology optimization?

Topology optimization can be described as a mathematical method which contributes to optimize the distribution of the material within defined constraints and minimizing the predefined cost function. This method can be used by mechanical or analysis engineer to minimize the amount of the used material and the strain energy of structures without losing their mechanical strength and their other mechanical properties.

In the topology optimization process, various topology optimization techniques can be obtained by using different optimization algorithms by considering the Computer Aided Design (CAD) concept, the Finite Element Analysis (FEA) concept and different production techniques. The use of CAD in topology optimization can make the first model of the product to be optimized. However, FEA can be used to observe the distribution of stresses throughout the model. Topology optimization can be done to remove areas of the part that do not adequately support the applied loads and do not undergo large deformation and therefore do not provide the overall performance of the part.

Based on these design problem requirements, various optimization algorithms can be used to remove the part of the material in the product that does not seem to support the applied load. In addition, topology optimization can be done to meet specific design goals and maintain design requirements and constraints.

The method can be continuously evaluated the structural stress distribution as it removes material to assess the resulting effects. That can be repeated through many individual steps until stable geometries are obtained according to the loadings and boundary conditions set up previously.

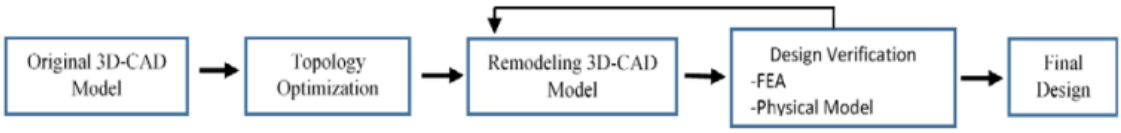

Figure 5.4 Topology optimized design process (Gebisa, A.W.,2017)

The design can be finalized in CAD software to obtain a stylish and manufacturable part by following the form created from the topology optimization method. As a result, the final optimized design can be validated using FEA to meet the design constraints to meet the overall performance of the product. (Tomlin M,2011)

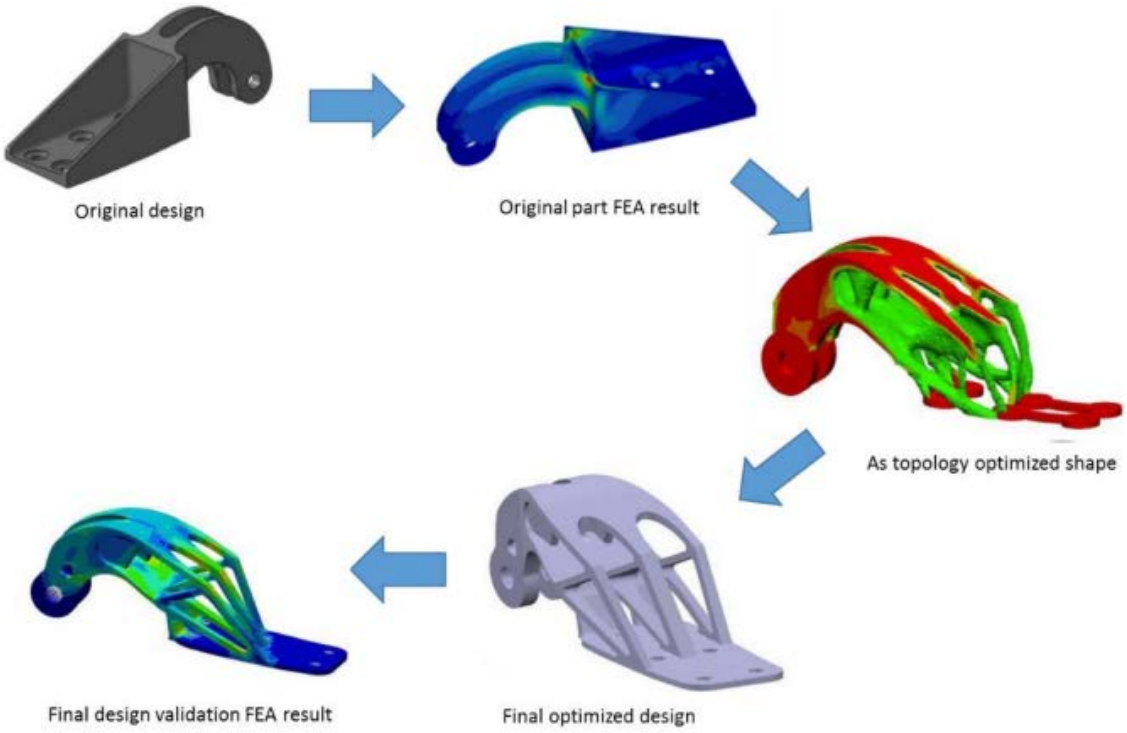

Figure 5.5 Topology optimization process (Gebisa, A.W.,2017)

Topology optimization in particular has some advantages in the design process. These are listed below.

- Manufacturing slight structures
- Creating a ready-to-manufacture design
- The high amount of material conservation
- Decreasing some physical tests which are related to mechanic
- Reducing physical prototype build

1.13.2 Formulation of the topology optimization problem

The formulation of the topology optimization ensures that the best solution is done correctly. These five steps are widely used in the formulation of the design optimization problem. (Gebisa, A.W.,2017)

1. Develop a topology optimization problem statement: The main purpose of this step is what will be achieved by optimization and the set of requirements can be clarified.
2. Data and information collection: All necessary information's can be collected in this step.

3. Identification/definition of design variables: In this step, the design variables that describe the system are identified and defined.
4. Identifying a criterion to optimize: In this step, the constraint to evaluate and stop the optimization process should be clarified. This criterion can be called objective functions that should be maximized or minimized depending on the design requirements.
5. Identifying constraints: In this step, constraints on the problem can be defined. They are deduced from resources and performance requirements.

Mathematically the optimization problem can be formulated as in equation below:

$$\text{Minimize : } f(x)$$

$$\text{Subject to : } g_i(x) \leq 0,\ i = 1, m$$

$$h_j\ (x) = 0,\ j = 1, p$$

$$x_k^l \leq x_k\ \leq x_k^u,\ k = 1, n$$

where;

$f(x)$ is an objective function to be minimized

g(x) and h(x) are inequality and equality constraints respectively.

m and p are a number of inequality and equality constraints separately.

x is a vector of design variables;

n is a total number of design variables;

x_k^l and x_k^u have been a lower and upper bounds of the k^{th} design variable x_k, respectively.

1.14 Modal Analysis

Modal analysis provides to determine the vibration characteristics (natural frequencies, the damping at natural frequencies, and mode shapes at natural frequencies) of a mechanical structure or component, whose parts show movement under the dynamic excitation. This modal analysis provides to reduce the noise emitted from the structure to the environment. It contributes to find out the reasons of the vibration that leads damage of the integrity of the structure.

Figure 5.6 illustrates the theoretical procedure of this analysis. First of all, the physical properties of the structure, usually as their stiffness value, mass, and damping characteristic are written in the modal analysis.

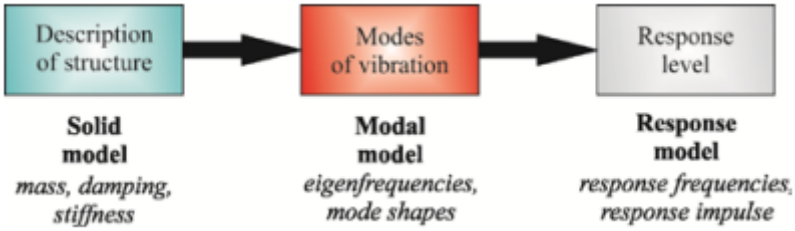

Figure 5.6 Theoretical procedure of vibration analysis (Lengvarský, P.,2013)

Then the theoretical modal analysis of the solid model causes the behaviour of the structure to be described in terms of vibration modes, and this is called the modal model. (Lengvarski, P.,2013). That model can be described as a set of natural frequencies with damping factor and natural mode vibration. This solution describes various methods of structure vibration.

After that, the response of the model, corresponding to its excitation and amplitude, is the next part of the theoretical procedural analysis. The model can describe a number of frequency response functions.

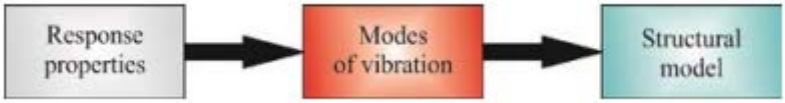

Figure 5.7 Experimental aim (Lengvarský, P.,2013).

This analysis can also be opposite direction; analysis starts with the response properties, which provides to understand the modal model properties. This method can be called the experimental procedure of vibration analysis and it is shown as in Figure 5.7.

In Figure 5.8, the general procedure for linking in modal analysis can be shown as below.

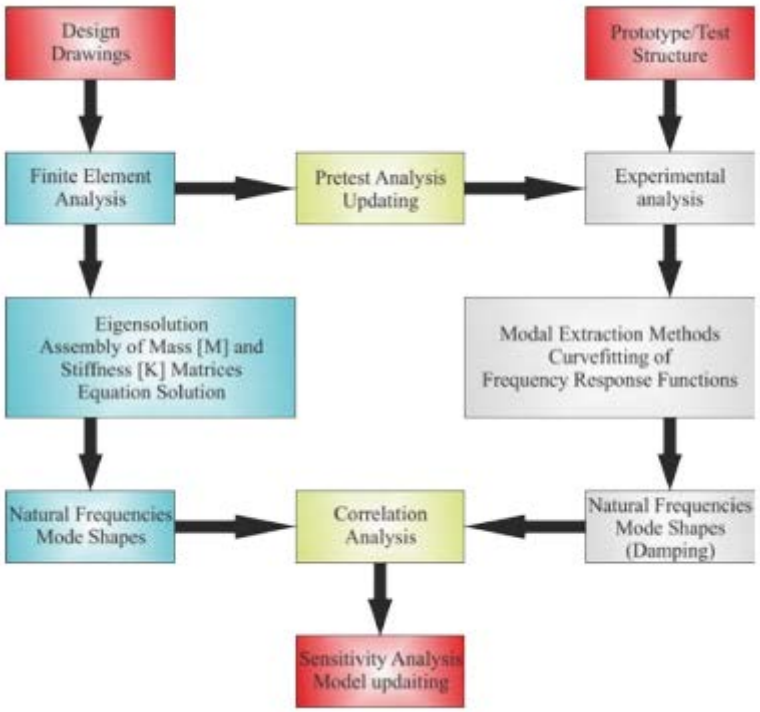

Figure 5.8 General procedure for modal analysis (Lengvarský, P.,2013)

CONCEPTUAL GIMBAL DESIGN

1.15 Design Requirements and Assumptions

In order for a product that is exposed to vibration to fulfill its intended use and to do this throughout its desired operational life, there are issues that need to be considered in the design process of this product, such as weight, dimension, material strength etc. In order to determine the size limits, the payload volume of the sample UAV mentioned in the introduction part of the thesis was taken into account. In Figures 6.1 and 6.2, the payload volume in the lower body of the UAV is shown as the top view and isometric view, respectively. In Figure 6.3, an imaginary volume was drawn, and the maximum dimensions of the gimbal were determined as 250x230x230 mm.

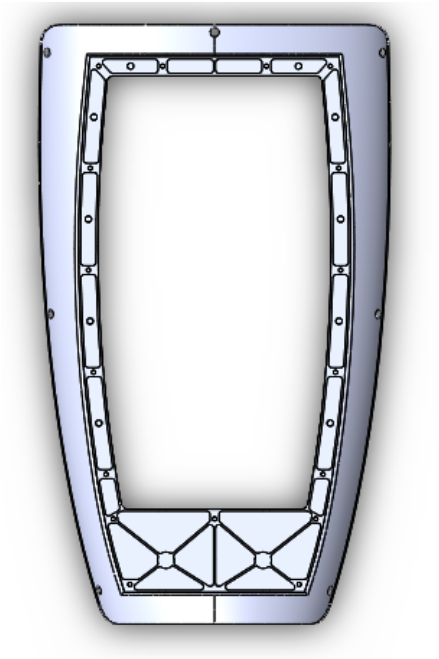

Figure 6.2 Top view of lower UAV body

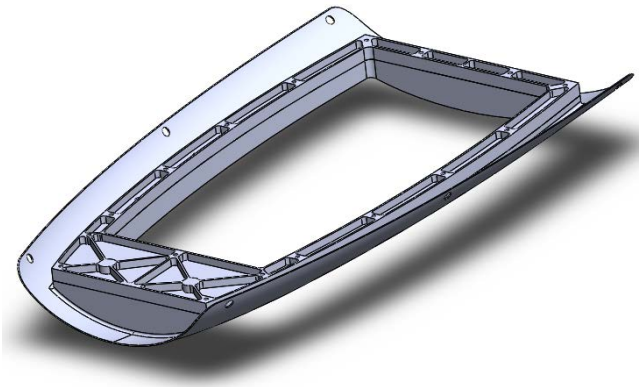

Figure 6.1 Isometric view of lower UAV body

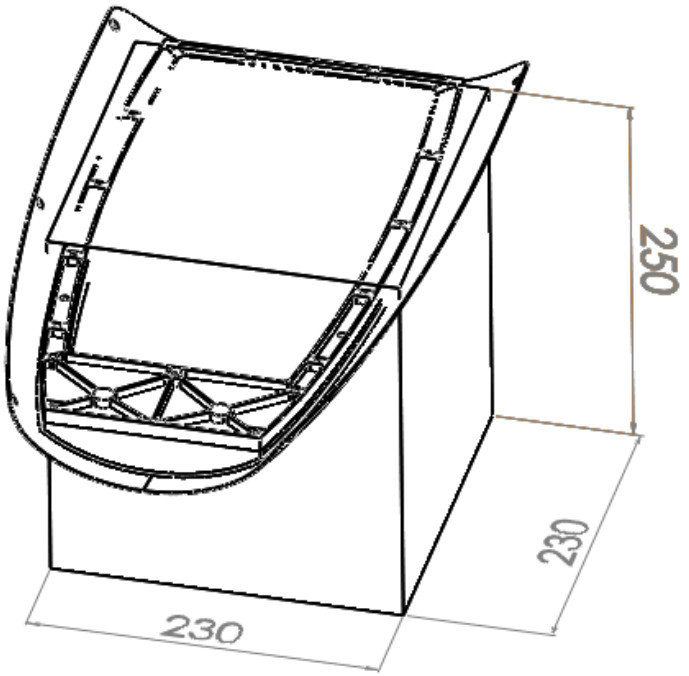

Figure 6.3 Payload volume (dimensions are mm)

After the general physical properties of the product are known, the source and characteristics of the vibration should be known. However, there is no vibration data and graph for the mini-UAV in the guidelines mentioned in the previous chapters.

FFT analysis was not performed as data was not collected by accelerometer within the scope of the thesis. Instead, the current mini-UAV vibrations in the literature were examined by doing a literature review.

1.15.1 Literature Review for Vibration Sources in Air Vehicles

We can collect the source of vibration in the aircraft in three main groups vibrations originating from the external environment, arising from the propulsion system of the aircraft, and vibrations arising from other functions of the aircraft.

Vibrations originating from the external environment are ground vibrations during taxi and take-off (Burström, L & Lindberg, L., 2006) and vibrations caused by aerodynamic forces during flight. (Liu, Y., 2020)

The type of thrust of the aircraft can cause a vibration environment. Turbofan jets or reciprocating engines are an important source of vibration for aircraft, even if they have different characteristics. Almost all propeller aircraft have propellers mounted at the front

of the fuselage or wing; it means that the airframe can be continuously affected by the wake propagating from each propeller blade. (Dunno, K., & Batt, G.,2009)

Vibration can also be caused by aircraft functions, containing the landing gear, operation of flaps, airbrakes, and other systems.

Since the gimbal designed within the scope of this thesis will not take images during the taxi, take-off, and landing phases of the UAV, only the cruise phase is taken into account during the modelling of the vibration to which the optical system will be exposed. During the cruise, vibrations caused by aerodynamic forces and the vibration of the UAV engine are effective. Since modelling the vibration caused by aerodynamic forces would be so comprehensive that it would be a thesis topic on its own, only engine-induced vibrations are examined in this thesis.

In the thesis named (Lai, Y. C., & Jan, S. S.,2011), the effect of the engine vibration of the mini UAV on the GPS system was investigated. The UAV mentioned in this thesis is an 80cc two-stroke gasoline engine with a 3.5 m wingspan. Vibration analysis of the UAV was performed with the FFT analysis method mentioned in chapter 5.1.

According to (Lai, Y. C., & Jan, S. S.,2011) Temporal information is lost in the conversion process, but in this study, the vibration frequency changes over time as the aircraft was operated under different flight conditions. Because of this, the Short Time Fourier Transform method was used to observe the temporal information in the frequency domain, and the dominant vibration frequency at different times during the flight was determined. If we look at the determined frequencies, it is seen that it is related to the engine speed and propeller speed and is between 100-150 Hz during the cruise.

When two more different studies are examined (Alsalaet, J.,2012), (Legriffon, I.,2016), the vibration caused by the engine speed and the propeller is dominant in the spectrum analysis. In addition, due to the event called blade pass frequency, vibration occurs not only in the propeller revolution but also in the frequency that corresponds to the multiplication of the propeller revolution with the number of propeller blades.

Engine and Propeller of mini-UAV

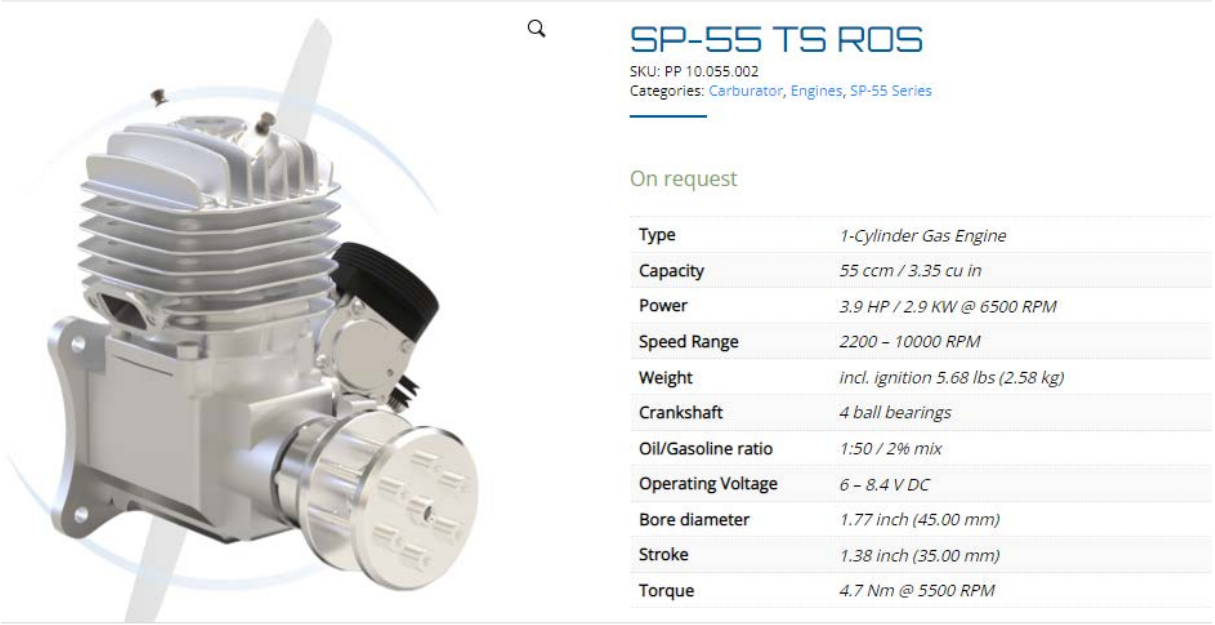

Figure 6.4 Example engine for mini-UAVs (skypower.online)

$$Frequency\ of\ Engine = \frac{9000Rpm}{60} = 150\ Hz$$

1.15.2 Design Requirements Summary

The design requirements of the gimbal are given in Tables 6.1 and 6.2.

Table 6.1: Design requirement and its physical properties

Necessary Properties	Numerical Value
Dimensions	Height=250 mm, Width=230 mm, Length=230 mm
Optical System Weight	1.5 kg
Gimbal Weight	< 5 kg
Yaw Angle	360°
Pitch Angle	-30° , +110°

Table 6.2: Design requirement and its vibration characteristics

Characteristics of Excitation Vibration	Type and Limitation
Vibration Type	Harmonic Base Excitation
Excitation Frequency	150 Hz
Required Isolation	97%
Max Static Deflection	0.3 mm
Vibration Type	Harmonic Base Excitation

1.16 Material Selection

When it comes to selecting the construction material for the system, there are several factors to consider. Because the weight of the gimbal is restricted to the entire weight the UAV can carry, the density of the materials is important. Second, the material's Young's modulus, and tensile strength are critical for avoiding deformations when working. Furthermore, because the system will work at different temperatures, the melting point and thermal conductivity should be addressed while selecting the material. Additionally, while choosing a material, the production time and method, pricing, and post-process of each material should be considered.

As a result of the literature review, it has been seen that mostly 6000 or 7000 series aluminium alloys are used in aviation parts. Its biggest advantage is that it is light and has sufficient strength. It is also easy to machine and suitable for various coating methods.

Table 6.3 Mechanical Properties of Materials

Material	Density (kg/m^3)	Yield Strength (MPa)
Aluminum alloy - 6061	2720	35
Aluminum alloy - 7050	2800	58

ISOLATION SYSTEM DESIGN CALCULATIONS

1.17 Choosing k_{eq} and c_{eq} Values for Isolation System and Spring Calculation

To choose right k_{eq} and c_{eq} value for our design, iterations can be needed. First of all, some necessary parameters can be used in the iterations:

$$\omega_n = \sqrt{\frac{k}{m}}$$

$$r = \frac{\omega}{\omega_n}$$

$$\zeta = \frac{c}{2\sqrt{km}}$$

After that, using transmissibility ratio, which means that the ratio of output to input right k and c values can be chosen easily.

$$\beta = \sqrt{\frac{1 + (2 * \zeta * r)^2}{(1 - r^2)^2 + (2 * \zeta * r)^2}}$$

Moreover, static deflection can also be considered to choosing k_{eq} and c_{eq} values

$$\delta = \frac{mg}{k}$$

Firstly, the iteration can be started with m= 1.5 kg (it is defined earlier in system requirements) and k_{eq}= 1000 N/m, and c_{eq}= 2 Ns/m. The iterations can be calculated using the Excel and listed below.

Table 7.1 Iteration to find k_{eq} and c_{eq} values for the system

Iteration Number	k_{eq} (N/m)	c_{eq} (Ns/m)	ζ	r	β	δ (mm)
1	1000	2	0.05164	48.67	0.0022	14.715
2	10000	2	0.01633	15.39	0.0047	1.4715
3	20000	5	0.02887	10.88	0.0101	0.7358
4	30000	8	0.03771	8.89	0.0154	0.4905
5	40000	15	0.06124	7.70	0.0236	0.3679
6	50000	20	0.07303	6.88	0.0306	0.2943

The iteration can stop after the six iterations because static deflection and transmissibility values are acceptable for system requirements. Also, the graph of 'Transmissibility vs r' can be seen in the appendix.

Our k_{eq} value is 50000 N/m and c_{eq} value is 20 Ns/m

After the finding k_{eq} and c_{eq} values. The springs are designed using spring design equations, which are equations 4.11, 4.13, 4.14 and 4.15.

Designing spring for our system

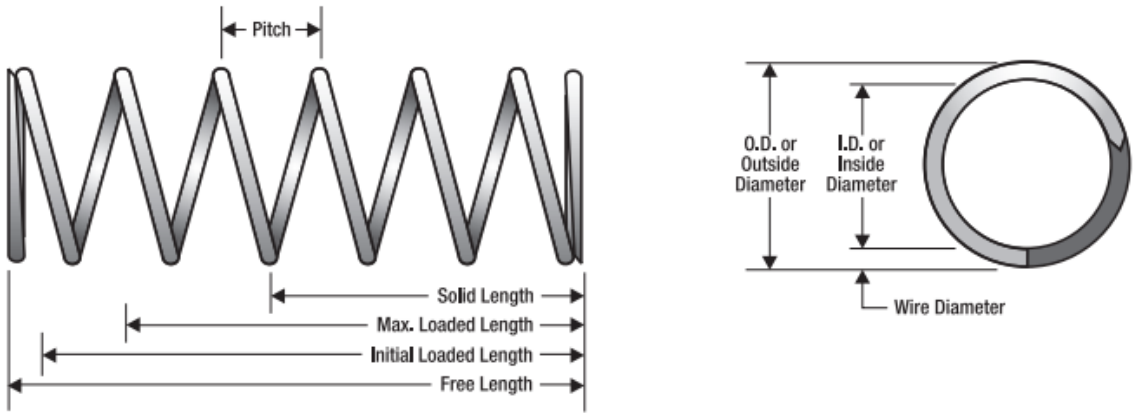

Figure 7.1 Spring dimensions (masterspring.com)

First of all, to choose right sizes for spring, the system requirements are considered, and the design will start some assumptions.

Requirements & Decisions

- Solid length (L_s) is chosen to be less than 29 mm.
- Spring rate (k_{eq}) is found 50000 N/m.
- The type of spring ends is square and ground.
- Four parallel springs are used.
- Spring wire is chosen Music wire A228. (G = 81 GPa).
- Force is chosen 100 N.

Using equation 4.11 ,4.12, 4.13, 4.14, 4.15, the inner diameter, outer diameter, and spring index can be chosen by iterations. These iterations can be shown in the Table below.

Table 7.2 Iteration to find wire diameter, outer diameter, and spring index

d(mm)	C	D(mm)	K_B	S_{sy}(MPa)	$\tau\ (MPa)$	n_s	N_a	N_t	L_s(mm)
2	4	8	1.385	1199.8	352.6	3.40	25.3	27.3	54.63
2	5	10	1.29	1199.8	411.9	2.91	13.0	15.0	29.92
2.2	5	11	1.29	1183.3	340.4	3.48	14.3	16.3	35.76
2.5	6	15	1.24	1161.5	302.7	3.83	9.4	11.4	28.44

After the four iterations, parameters are sufficient for the system's requirements. These values can be solved in analytically below.

$$S_{sy} = 0.60\ \frac{2211}{2.5^{0.145}} = 1161.5\ MPa$$

C is chosen 6 and outside diameter becomes D = Cd= 15 mm from equation 4.11.

$$K_B = \frac{4C + 2}{4C - 3} = 1.238$$

$$\tau = K_B \frac{8FD}{\pi d^3} = 1.238 \frac{8(100)(15)}{\pi(2.5)^3} = 302.7\ MPa$$

$$n_s = \frac{1161.5}{302.7} = 3.83\ (\ reasonable\ and\ safe\ )$$

4 parallel springs are used in the design. As k_{eq} was found as 50000 N/m after the iteration. Each spring's rate becomes 12500 N/m using equation 4.20.

Number of active coils can be found as using equation 4.15 :

$$k = \frac{Gd^4}{8D^3N}$$

$$12.5 = \frac{(81x\ 10^3)\ 2.5^4}{8\ 15^3 N} \quad \rightarrow N = 9.4\ coils$$

$$N_t = N_a + 2 = 9.4 + 2 = 11.4\ coils$$

Using Table 4.1, the solid length of the spring becomes

$$L_s = d * N_t = 2.5 * 11.4 = 28.44\ mm$$

Finally, these parameters can be summarized in the Table below.

Table 7.3 Summary of physical properties of spring

Inside diameter	**Outside diameter**	**Number of Active Coil**	**Number of Total Coil**	**Solid Length**	**Type of spring wire**	**Spring Rate**	**Shear modulus of elasticity**
2.5 mm	15 mm	9.4 Coils	11.4 Coils	28.44 mm	Music wire A228	12500 N/m	81 GPa

1.18 Analytical Solution of The Equation of Motion

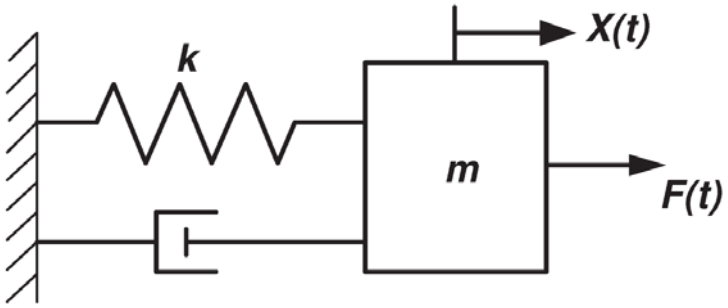

Figure 7.2 A Mass- Spring- Damper System with External Force (Al-Salti, N., Karimov, 2016)

The forced vibrations of a SDOF when a linear displacement can be chosen as the generalized coordinate is governed by equation 3.8.

$$m_{eq}\ddot{x} + c_{eq}\dot{x} + k_{eq}x = F_{eq}(t)$$

The general solution can be written as using equation 3.9.

$$x(t) = x_h(t) + x_p(t)$$

After some requirements (Table 6.1) and iterations (k_{eq} and c_{eq}) value of these physical properties can be listed below:

$m_{eq} = 1.5\ kg$

$c_{eq} = 20\ \ Ns/m$

$k_{eq} = 50000\ N/m$

$F_{eq} = 500\sin(942.48t)\ N$

After determining the values of properties, homogenous solution can be solved firstly.

$$1.5\,\ddot{x} + 20\,\dot{x} + 50000\,x = 0$$

The characteristic equation becomes:

$$1.5\,r^2 + 20\,r + 50000 = 0$$

Roots can be found as :

$$r_{1,2} = -\frac{20}{3} \pm i\ \frac{20\sqrt{749}}{3}$$

Hence, the homogenous solution can be found using differential equation's knowledge :

$$x_h(t) = e^{\left(-\frac{20}{3}\right)t}\left(C_1\cos\left(\frac{20\sqrt{749}}{3}t\right) + C_2\sin\left(\frac{20\sqrt{749}}{3}t\right)\right)$$

$$x_h(t) = e^{\left(-\frac{20}{3}\right)t}\left(C_1\cos(182.452t) + C_2\sin(182.452t)\right)$$

Then, the particular solution can be determined using the method of undetermined coefficients method :

$$x_p(t) = Acos(942.48t) + Bsin(942.48t)$$

The first and second derivatives of particular solution can be found as :

$$\dot{x_p}(t) = (-942.48)\ A\ sin(942.48t) + (942.48)\ B\ cos(942.48t)$$

$$\ddot{x_p}(t) = -(942.48)^2\ A\ cos(942.48t) - (942.48)^2\ B\ sin(942.48t)$$

First and second derivative can be put inside the damper-spring-mass differential equation:

$$1.5\left(-(942.48)^2\ A\ cos(942.48t) - (942.48)^2\ B\ sin(942.48t)\right)$$
$$+ 20\left((-942.48)\ A\ sin(942.48t) + (942.48)\ B\ cos(942.48t)\right)$$
$$+\ 50000\ (Acos(942.48t) + Bsin(942.48t)) = 500\sin(942.48t)$$

$cos(942.48t)$ and $sin(942.48t)$ terms are gathered separately

$$cos(942.48t)\ \ (\text{-}1.5\ (942.48)^2\ A + 20\ ((942.48)\ B + 50000\ A) = 0$$

$$sin(942.48t)(-1.5(942.48)^2\ B - 20\ \left((942.48)\ A + 50000\ B\right) =\ 500\ sin(942.48t)$$

Then A and B coefficients can be found as :

$$\text{A = -5.73 x}10^{-6} \quad \& \quad \text{B = - 3.90 x}10^{-4}$$

After that, particular solution can be found as :

$$x_p(t) = -5.73\text{x}10^{-6}cos(942.48t) -\ 3.90\ \text{x}10^{-4}\ sin(942.48t)$$

The general solution can be written as :

$$x(t) = e^{\left(-\frac{20}{3}\right)t}\ (C_1\cos(182.452t) + C_2\sin(182.452t)) - 5.73\text{x}10^{-6}cos(942.48t)$$
$$-\ 3.90\ \text{x}10^{-4}\ sin(942.48t)$$

To find C_1 and C_2 ,boundary conditions are put inside the general solution. Our boundary conditions are :

$$x(0) =\ 3\ \text{x}10^{-4}$$

$$\dot{x(0)} =\ -10^{-3}$$

$$x(0) =\ C_1 + -5.73\text{x}10^{-6} =\ 3\ \text{x}10^{-4} \quad \rightarrow \quad C_1 = 3.06\ \text{x}10^{-4}$$

$$\dot{x}(t) = -\frac{20}{3}\ e^{\left(-\frac{20}{3}\right)t}\ (C_1\cos(182.452t) + C_2\,\text{sın}(182.452t)) +$$

$$e^{\left(-\frac{20}{3}\right)t}\ (-182.452\ C_1\sin(182.452t) + (182.452)C_2\cos(182.452t)) +$$
$$(942.48)\ 5.73\text{x}10^{-6}\sin(942.48t) - (942.48)\ 3.90\ \text{x}10^{-4}\ cos(942.48t)$$

$$\dot{x}(0) = -\frac{20}{3}C_1 + (182.452)C_2 - (942.48)\ 3.90\ \text{x}10^{-4} = -10^{-3}$$

$$C_2 = 0.00202$$

Finally the general solution is :

$$x(t) = e^{\left(-\frac{20}{3}\right)t}\ (3.06x10^{-4}\cos(182.452t) + 0.00202\sin(182.452t)) \\ - 5.73\text{x}10^{-6}cos(942.48t) - \ 3.90\ \text{x}10^{-4}\ \ sin(942.48t)$$

This equation can be plotted in Matlab by choosing t=0:0.01:2

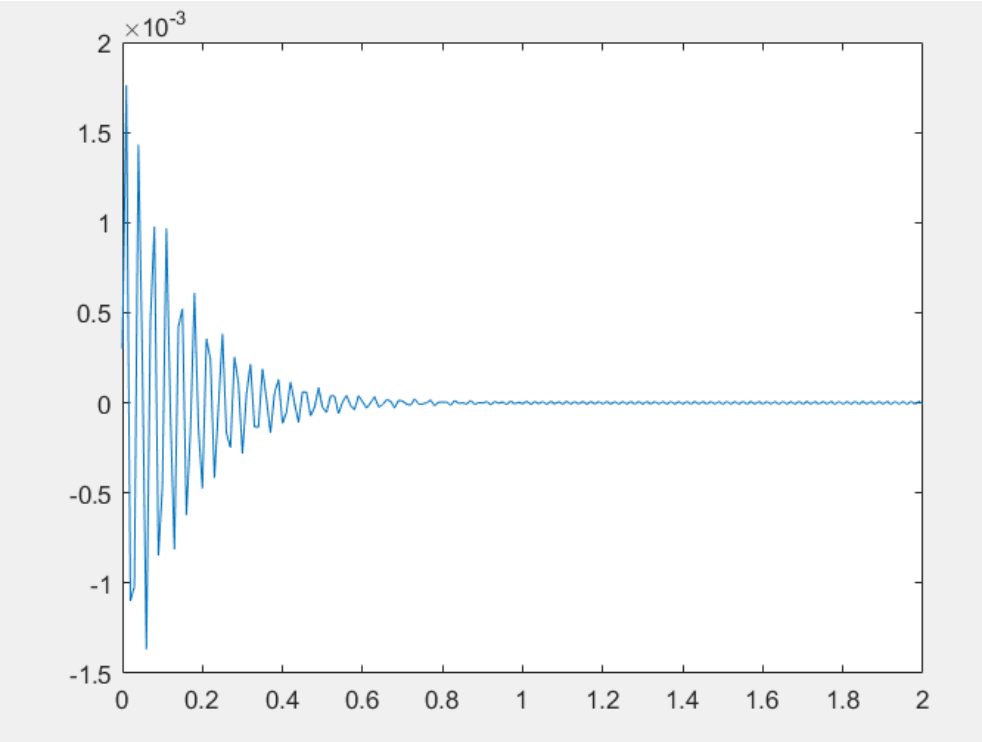

Figure 7.3 Graph of forced vibration equation solution by hand

Moreover, this mass-spring-damper equation can also be solved in Matlab differential equation solver (its code is in the appendices).

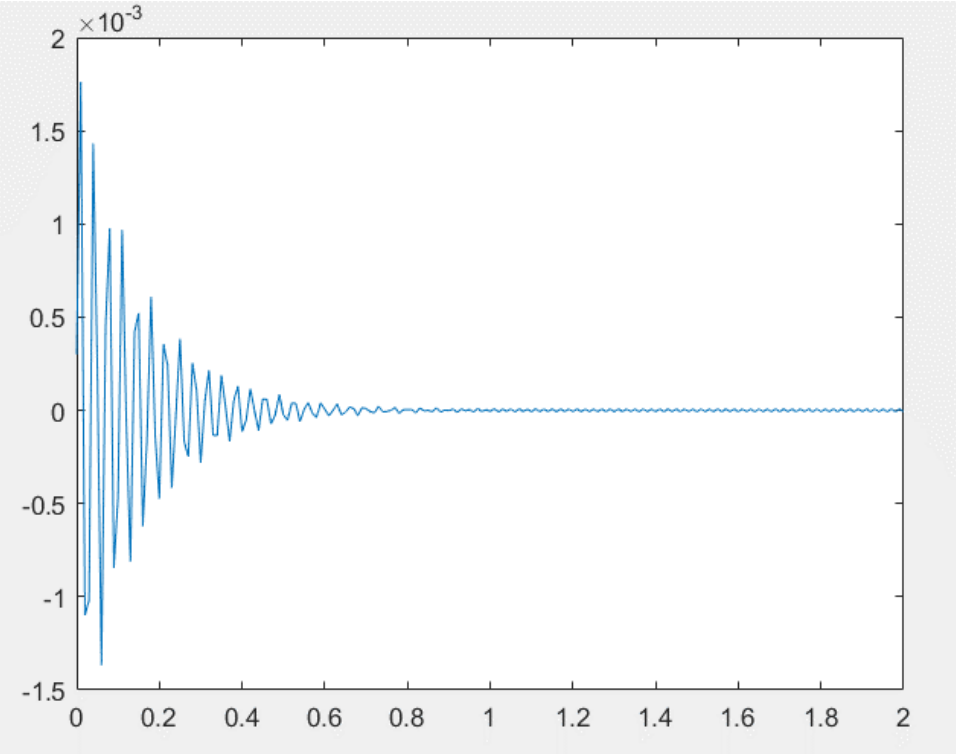

Figure 7.4 Graph of forced vibration equation solution by Matlab

As it can be seen, these graphs are similar. It means that our system can be isolated successfully in a few seconds, and it can be verified by Matlab codes.

PAN YOKE CRITICAL DESIGN AND RESULTS OF MODAL ANALYSIS

1.19 Pan Yoke Design

The dimensions of the optical ball containing the cameras were specified as a design requirement, and the dimensions are shown in Figure 8.1. The center of gravity is at the same point as the geometric center, and the weight is 1.5kg as mentioned before. The shaft on the axis of the optical ball was used as the axis of the tilt movement. Since the drive system, which provides the tilt motion, will prevent the design of the isolator, it has been decided first of all how the drive system will be. The three mechanisms considered to move the shaft are gear mechanisms, drive belt mechanisms, or direct drive motor systems. Gear systems are parts that both cause vibration and can be damaged as a result of vibration. Therefore, the gear mechanism is not considered in the design.

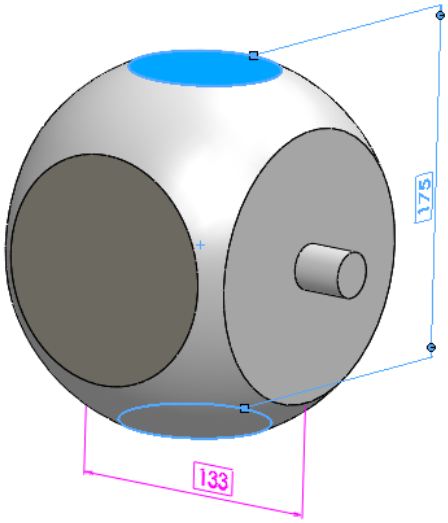

Figure 8.1 Optic ball dimensions

When using the drive belt mechanism, the motor is placed in the area marked with yellow in Figure 8.2. Thus, the small volume of the piece that needs to be fit into the small area shown in red in Figure 8.2 was seen as an advantage, and the first design was made. In addition, the belt drive system has the ability to absorb some vibration, so when starting the design, it was thought that the elastic structure could be used as a part of the isolator system. The simple concept design of this system is shown in Figure 8.3. After this design, the disadvantages of the system were evaluated, and it was thought that the area to be covered by the pulley dimensions in the yoke would be a lot. In addition, the elastic

structure of the belt will often exhibit nonlinear behavior. The stiffness and length of the belt may change due to the effect of heat and cold during its operational life. Therefore, the advantages and disadvantages of the third alternative direct drive motor system have been started to be considered.

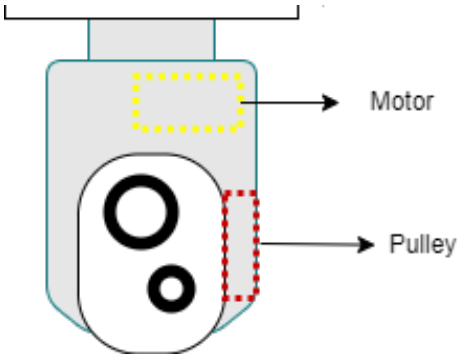

Figure 8.2 Drive belt mechanism concept layout

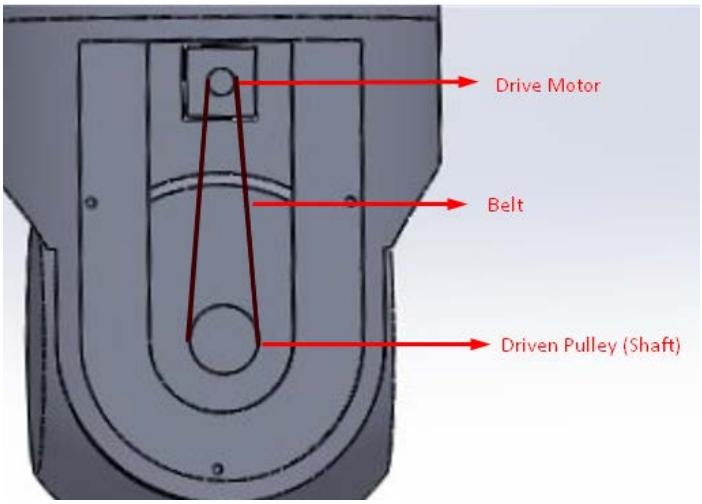

Figure 8.3 Drive belt mechanism CAD design

Since the direct drive motor will be directly connected to the shaft, the problems caused by the failure of the different elements are eliminated, and there are no problems such as gearbox backlash, and belt compliance. As a disadvantage, such motors can overheat and the heat inside the gimbal can damage the electronics. For this, cooling systems can be considered in gimbal design, but those parts are not within the scope of this thesis. In general, when focusing on the vibration problem, the direct drive motor is thought to be advantageous, and the design is shown in Figure 8.4.

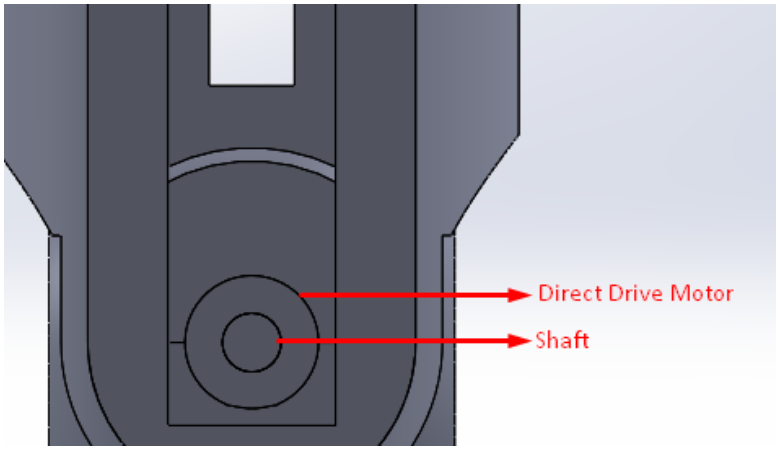

Figure 8.4 Layout of the direct drive motor

A bracket was designed to hold the motor connected to the shaft, and springs whose stiffness values were calculated analytically in the previous chapters of the thesis were placed between the bracket and the yoke. In addition, since the system is modeled as 1 DOF in the analytical solution, the constraints to ensure this have been taken into account in the design. The model in Figure 8.5 and the sliding mechanism in the design in Figure 8.5 indicate this.

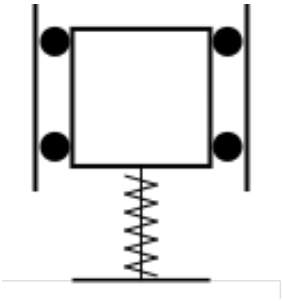

Figure 8.5 One DOF spring-mass model

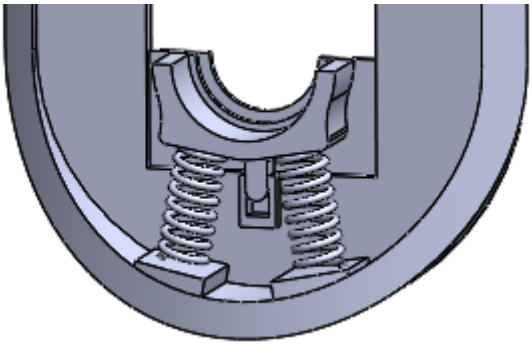

Figure 8.6 Motor bracket and springs layout

Since the stiffness value of the springs used in this design is much lower than the stiffness value of the aluminum yoke piece, it was thought that the yoke would not be affected by resonance at low frequencies, and only the optical ball would resonate. To analyze the validness of this hypothesis, the first modal analysis was carried out, and the results are shown in Figure 8.7.

The natural frequency, which was calculated as 29.05 Hz analytically, was found to be 22.87 Hz in Ansys (1st mode longitudinal axis of spring). One of the reasons for this, weighs are assumed in the analytical solution was 1.5 kilograms due to the weight of the optic ball. However, during the analysis, the motor that moves the optical system and the weight of the brackets holding these motors are added to the system. When the weight of the motors and brackets, which are approximately 400 grams, is taken into account in the analytical solution, the natural frequency is obtained as 25.81 Hz.

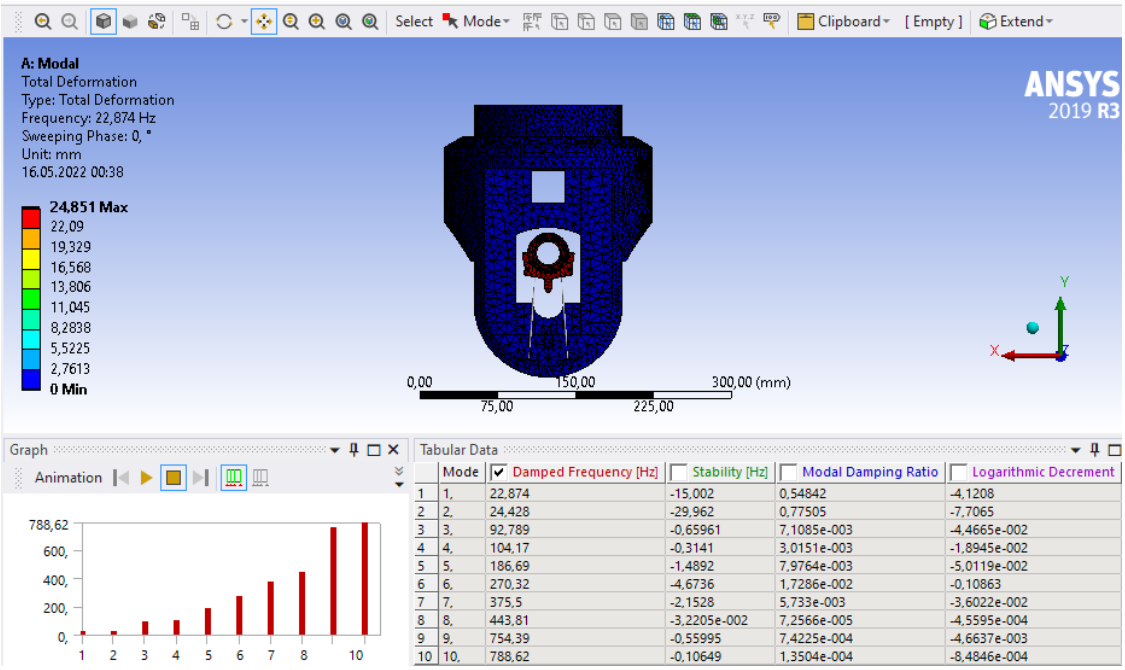

Figure 8.7 Modal analysis results of first design gimbal

In the continuation of the design, as a result of the first modal analysis to guide the design stages, it was seen that the first three mode shapes were directly related to the movement of the spring and optical system. As it can be seen in Figure 8.7 natural frequencies of modes 3,4 and 5 are close the base excitation frequency, which is 150 Hz. This design was analyzed without the yoke cover. When Figure 8.9 is examined to see the effect of the yoke cover, it is seen that the first three modes remained almost the same, while the

frequencies in the other modes increased. However, still close to the 3rd and 4th mode base excitation frequency. As a result of this modal analysis, some changes in the design are needed to move away from the base frequency. These needed changes can be like that increasing the stiffness of the structure or changing mass.

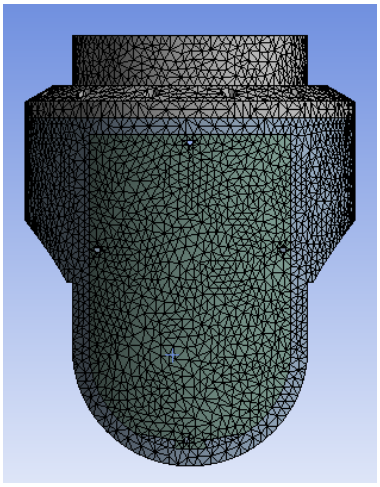

Figure 8.8 Mesh of the gimbal with cover

Tabular Data

	Mode	Damped Frequency [Hz]	Stability [Hz]	Modal Damping Ratio	Logarithmic Decrement
1	1,	22,844	-15,033	0,54971	-4,1346
2	2,	24,356	-29,924	0,77557	-7,7195
3	3,	93,358	-0,6612	7,0821e-003	-4,45e-002
4	4,	198,72	-2,4256e-002	1,2206e-004	-7,6692e-004
5	5,	276,65	-5,0045	1,8087e-002	-0,11366
6	6,	459,29	-0,32269	7,0258e-004	-4,4144e-003
7	7,	470,35	-9,3133e-003	1,9801e-005	-1,2441e-004
8	8,	674,12	-0,49384	7,3257e-004	-4,6028e-003

Figure 8.9 Modal analysis results of the gimbal with cover

In addition, the rotational movement of the third mode can be seen in Figure 8.10, and its frequency is 92.358 Hz. This means that the design cannot be modeled as in Figure 8.5. In order to change this mode, the upper bracket was added to the motor and the sliding movement was supported from the upper part. The new design is shown in Figure 8.11.

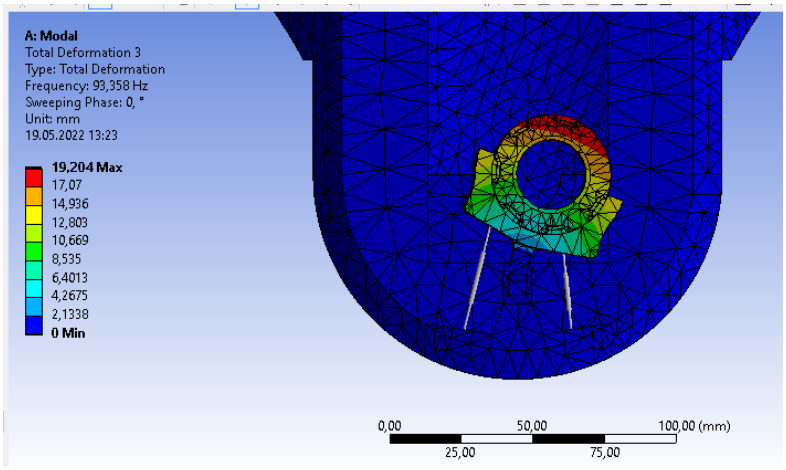

Figure 8.10 Third mode shape of the first design

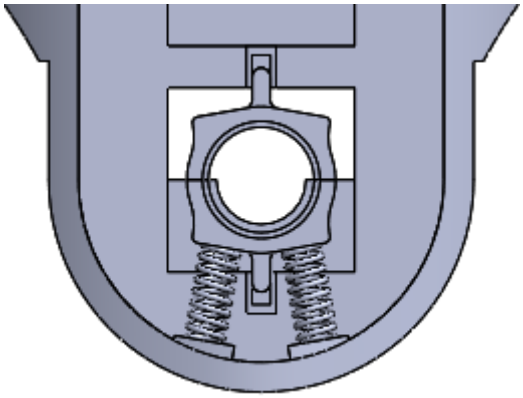

Figure 8.11 New design with the upper bracket

After adding the upper bracket, it was aimed to reduce the weight by making topology optimization since excess weight is an important problem in aircraft. After the static analysis, the result in Figure 8.12 (a) was obtained using the Ansys topology module. Considering this result and considering the manufacturability of the part, Figure 8.12 (b) was designed with Solidworks. After this stage, the modal analysis of the yoke was repeated several times, and design changes were made to increase the lowest natural frequency and not to increase the mass much.

As a result of the first modal analysis after the topology optimization, the lowest mode was obtained as 171.61 Hz. Later, as can be seen in Figure 8.12 (c), two ribs were added to the design to increase the rigidity of the part, and according to the analysis made in Figure 8.13, its natural frequency was determined as 186.3 Hz.

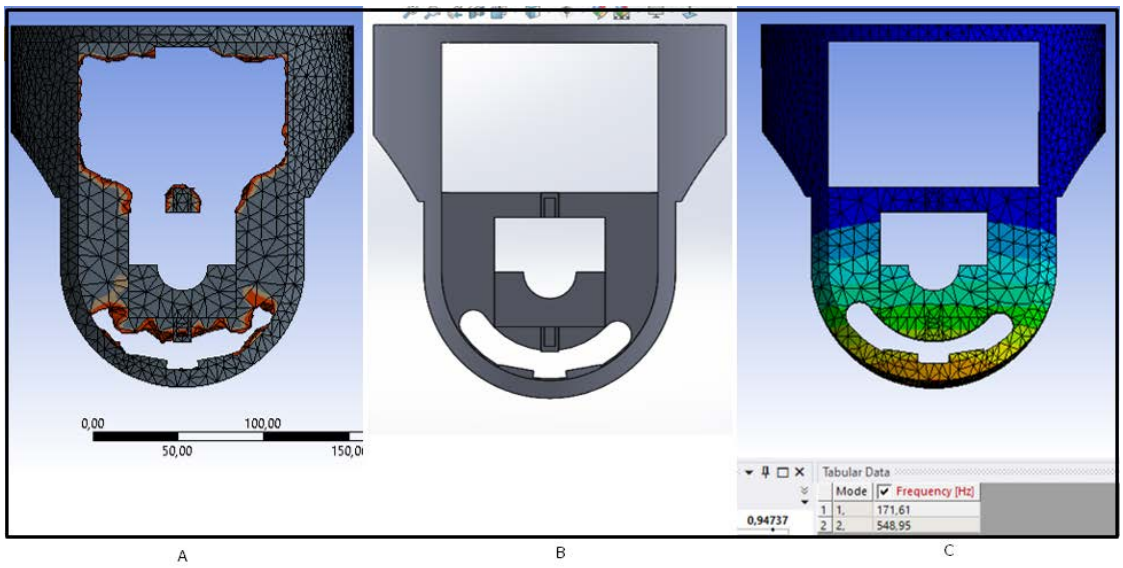

Figure 8.12 Topology optimization result (A), CAD design (B), modal analysis (C)

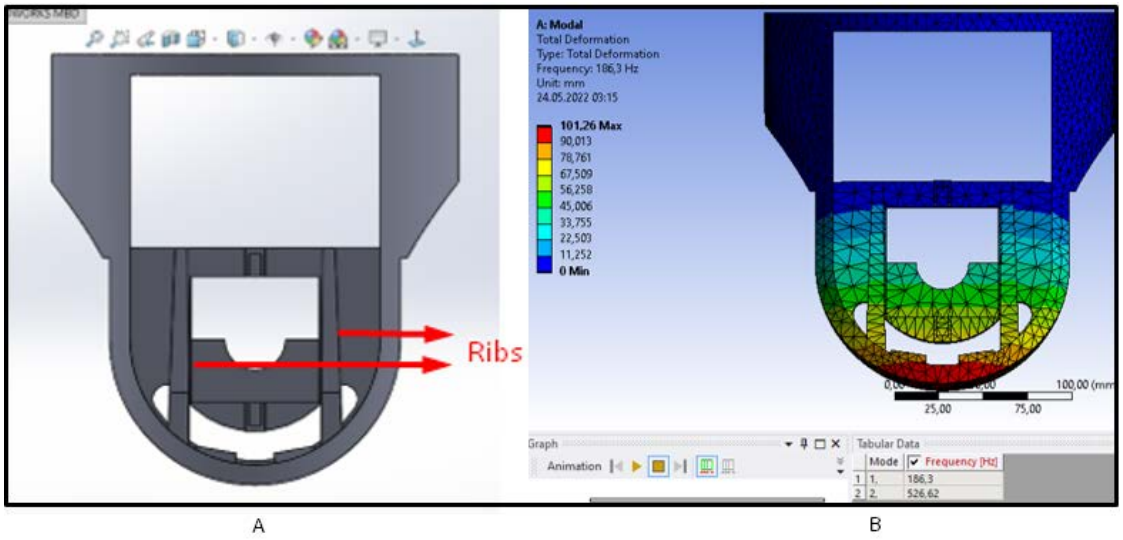

Figure 8.13 CAD design with ribs (A) and its modal analysis (B)

Finally, the design in Figure 8.14 has been made considering that thickening the yoke mid-section at the same level with the top of the motor bracket, which is in contact with the yoke, will increase the natural frequency. While making this design, it was thought that rain, dust or turbulent air could enter through the gap between the optical ball and the yoke, so as a result of topology, no holes were drilled on the part instead the wall thickness was thinned where holes.

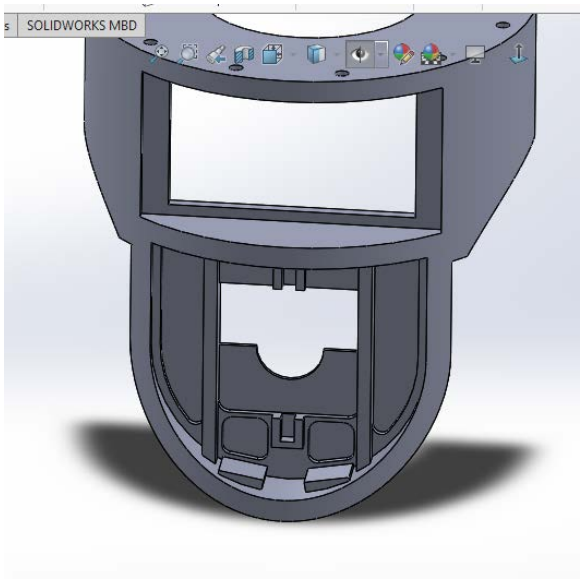

Figure 8.14 Mid-section thickened design

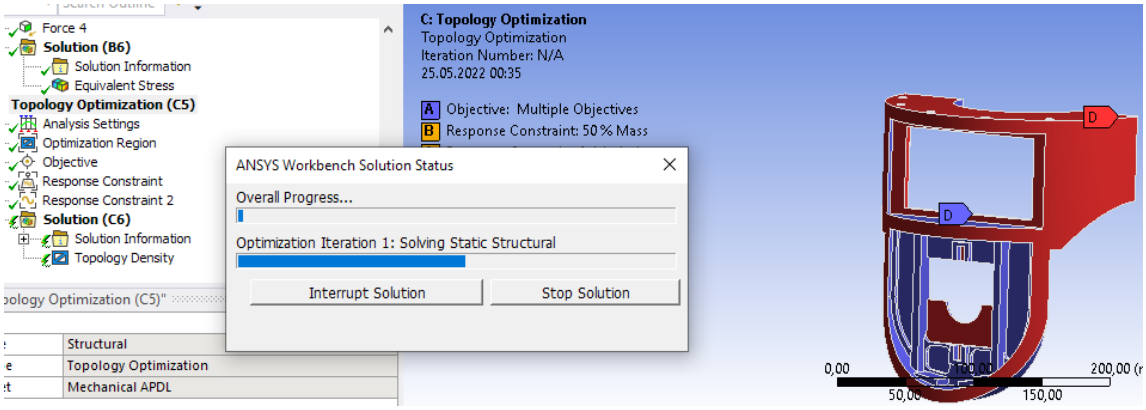

Figure 8.15 Topology optimization of mid-section thickened design

In addition, although the topology analysis with only mass reduction objective function was performed in the previous analyses, the natural frequency value was added as a constraint function to this design. Thus, while maintaining the natural frequency value reached by step-by-step changes, the mass was reduced. The result of the topology giving the final design is shown in Figure 8.16 (a), and the final design of the yoke, which is suitable for manufacturability, is shown in Figure 8.16 (b). The weight change as a result of topology optimization between the first design with acceptable natural frequency values and the final design is approximately 133 grams and is shown in Figure 8.17. Also, the final design of whole gimbal assembly is shown in Figure 8.18.

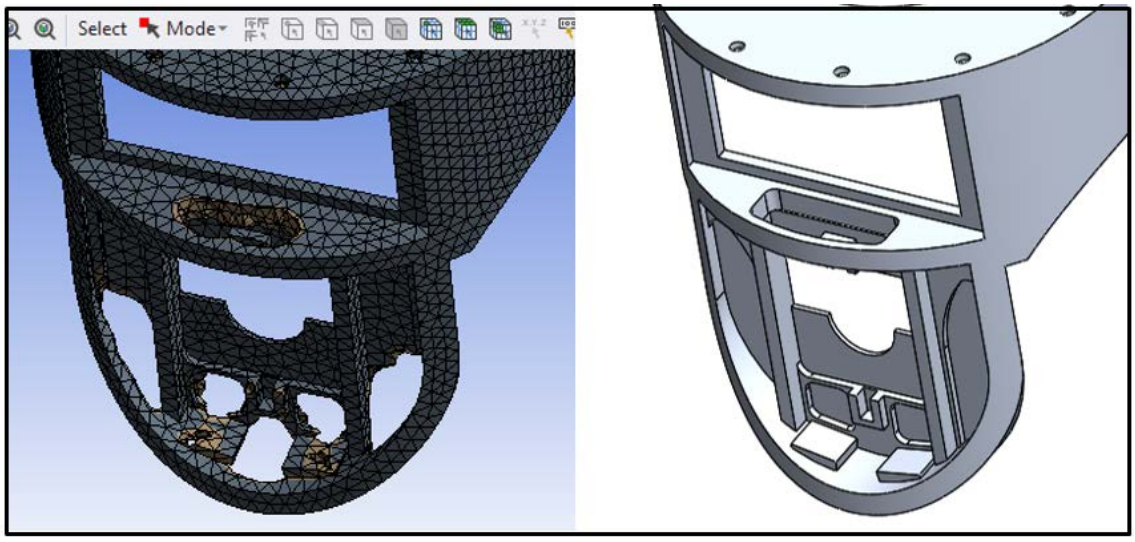

Figure 8.16 Latest topology (A) and CAD design based on this analysis (B)

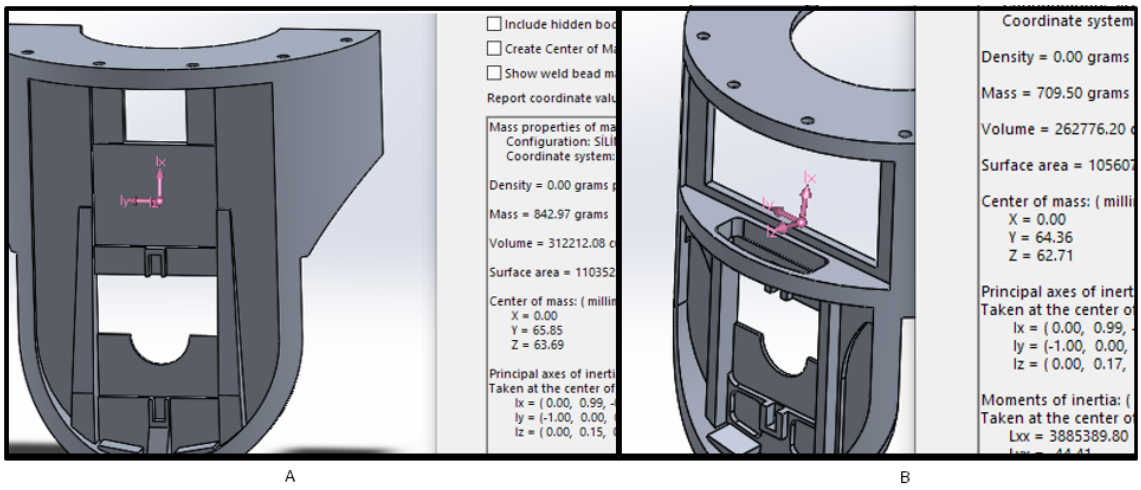

Figure 8.17 Weight of first acceptable design (A) and weight of final design (B)

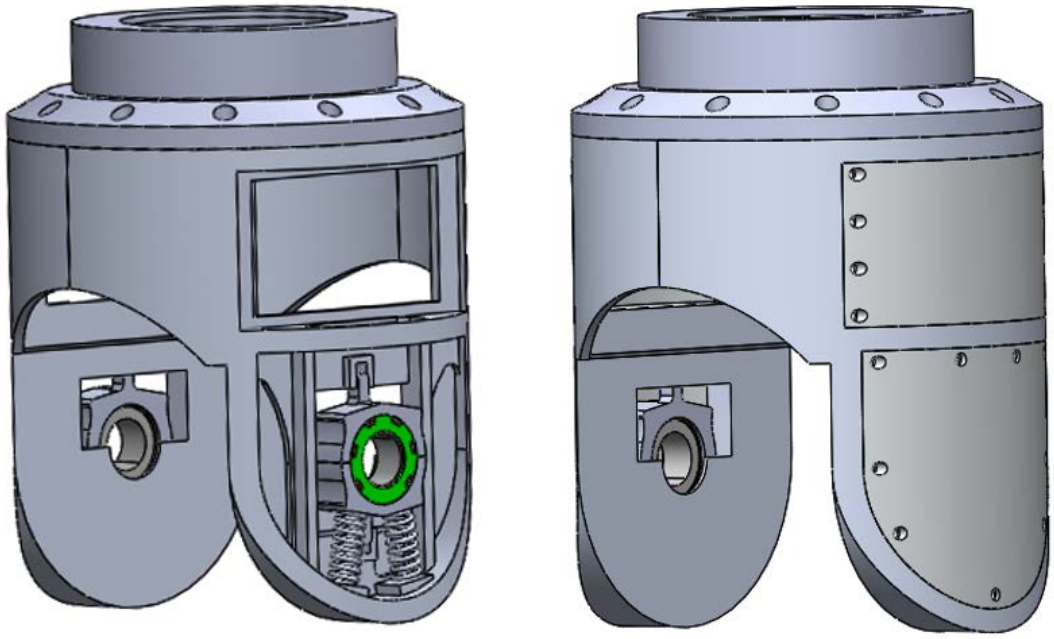

Figure 8.18 Final gimbal design without cover and with cover

1.20 Modal Analysis of Final Design

In the analyzes mentioned in the design part, an average mesh size was chosen for rapid analysis. In this part of the thesis, the final design will be analyzed and how the results obtained relate to mesh quality, and size will be examined. If the changes in the natural frequencies obtained by changing the mesh are small, it can be assumed that the natural frequency values we obtain will converge to a value.

After the reaching final design mesh independency of the analysis can be controlled. That is why, three different mesh sizes are chosen. These mesh sizes are 7mm, 6mm, and 5mm. The natural frequency values of the final design obtained with different meshes are shown in Table 8.1.

Tabular Data

	Mode	Damped Frequency [Hz]	Stability [Hz]	Modal Damping Ratio	Logarithmic Decrement
1	1,	22,673	-14,647	0,54261	-4,0588
2	2,	24,649	-28,21	0,75303	-7,1908
3	3,	388,24	-0,15526	3,9991e-004	-2,5127e-003
4	4,	474,11	-1,48e-002	3,1216e-005	-1,9613e-004
5	5,	474,12	-0,15224	3,2109e-004	-2,0175e-003
6	6,	540,6	-4,3975e-003	8,1345e-006	-5,111e-005

Figure 8.19 Modal analysis results of the final design with 7mm mesh size

Tabular Data

	Mode	Damped Frequency [Hz]	Stability [Hz]	Modal Damping Ratio	Logarithmic Decrement
1	1.	22,673	-14,647	0,54261	-4,0588
2	2.	24,649	-28,21	0,75303	-7,1908
3	3.	385,91	-0,15583	4,0379e-004	-2,5371e-003
4	4.	472,03	-7,224e-002	1,5304e-004	-9,6158e-004
5	5.	472,14	-9,4457e-002	2,0006e-004	-1,257e-003
6	6.	538,43	-4,5523e-003	8,4547e-006	-5,3122e-005
7	7.	679,58	-0,43993	6,4736e-004	-4,0675e-003

Figure 8.20 Modal analysis results of the final design with 6mm mesh size

Tabular Data

	Mode	Damped Frequency [Hz]	Stability [Hz]	Modal Damping Ratio	Logarithmic Decrement
1	1.	22,673	-14,647	0,54261	-4,0588
2	2.	24,65	-28,21	0,75303	-7,1908
3	3.	383,35	-0,15544	4,0549e-004	-2,5477e-003
4	4.	468,34	-1,9076e-003	4,0731e-006	-2,5592e-005
5	5.	470,49	-0,16517	3,5105e-004	-2,2057e-003
6	6.	535,83	-4,8088e-003	8,9745e-006	-5,6389e-005
7	7.	676,76	-0,43985	6,4993e-004	-4,0836e-003

Figure 8.21 Modal analysis results of the final design with 5mm mesh size

Table 8.1 Effect of the mesh size on the natural frequencies

Mode	Mesh Size 7 mm Frequency (Hz)	Mesh Size 6 mm Frequency (Hz)	Mesh Size 5 mm Frequency (Hz)
1	22.673	22.673	22.673
2	24.649	24.649	24.65
3	388.24	385.91	383.35
4	474.11	472.03	468.34
5	474.12	472.14	470.49
6	540.6	538.43	535.83

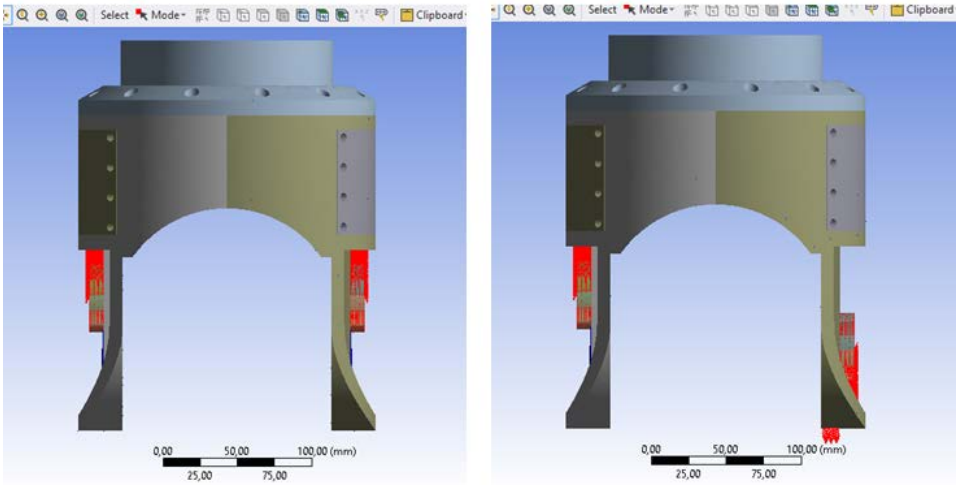

Figure 8.22 First mode shape 22.673 Hz (left) and second mode shape 24.65 Hz (right)

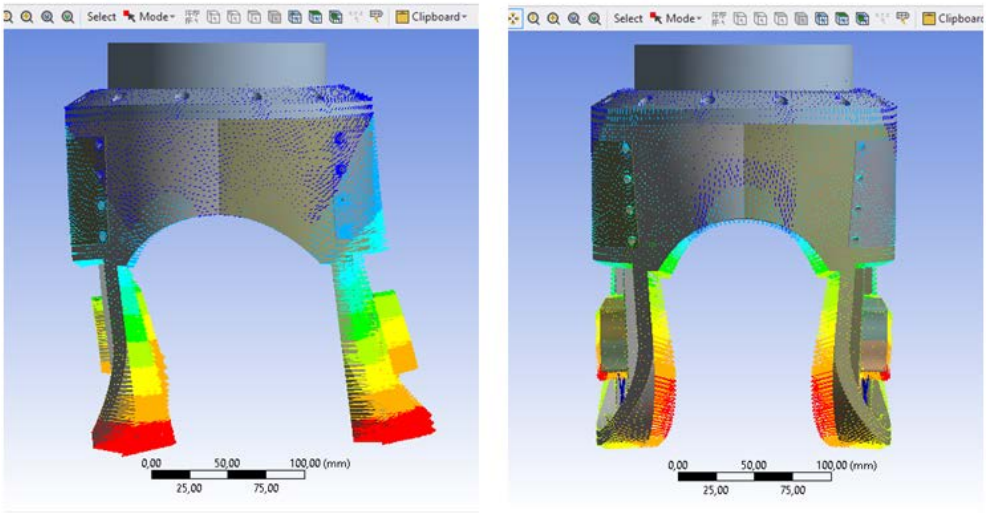

Figure 8.23 Third mode shape 383.35 Hz (left) and fourth mode shape 468.34 Hz (right)

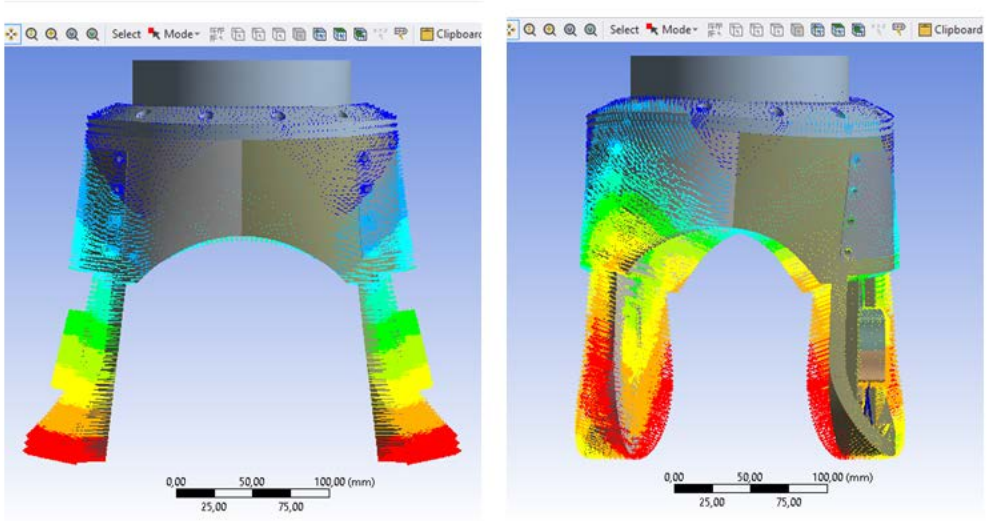

Figure 8.24 Fifth mode shape 470.49 Hz (left) and sixth mode shape 535.83 Hz (right)

EVALUATION OF THE CURRENT WORK FROM MUDEK PERSPECTIVE

1.21 Economic Analysis

One of the main concerns of engineering is the cost. First of all, york is manufactured from aluminium material. This metal not only has a lower price but also has strength values that can meet the required stress values for the design. Moreover, the york is subjected to the topology optimization process. This topology optimization process provides material savings by removing parts with negligible stress values. Furthermore, the programme of TUBITAK 2209/A Student Research Project Supports support scholarship for our project. Using this scholarship, we upgraded our computers to achieve better and more quickly analysis result.

1.22 Real-Life Conditions

Our project is done on the computers. We make some calculations to achieve safe design. Then the design was drawn on CAD Software. Then, static structural, topology optimization, and modal analysis is done on ANSYS Software. These operations are sensible, but it mostly depends on the theoretical approach. We didn't make experience in real life. If we apply our project on real life, the design, which was obtained by theoretical will be made in aluminium york casting. Then, the design is exposed to based excitation frequency in the experiment. Then amplitude is measured by the amplitude measurement device. At the end, we can observe the theoretical results and experimental measurements are similar or not.

1.23 Producibility

The manufacturability is a very important detail in the design. In the CNC Machine or other machines, all designs cannot be manufactured because some designs are more complex and not realistic. For example, in our design, after the topology optimization process, the outer line of the design becomes jagged. That is why, we made the same changes to the outer line to make it easier to produce.

1.24 Constraints

Constraints are the key of the design. All calculations or assumptions can change in accordance with the constraints. In our design, our system constraints are mass of the gimbal should be less than 4.5 kg, static deflection less than 0.3 mm, and transmissibility ratio should be smaller than 0.03 at the base excitation frequency is 150 Hz. Let the natural frequencies of our design stay away from the base frequency as much as possible. While doing this, they should not exceed the acceptable static deformation value and the transmissibility ratio value.

SWOT ANALYSIS

The SWOT Analysis of passive vibration isolation system design of UAV EO/IR Gimbal is shown below.

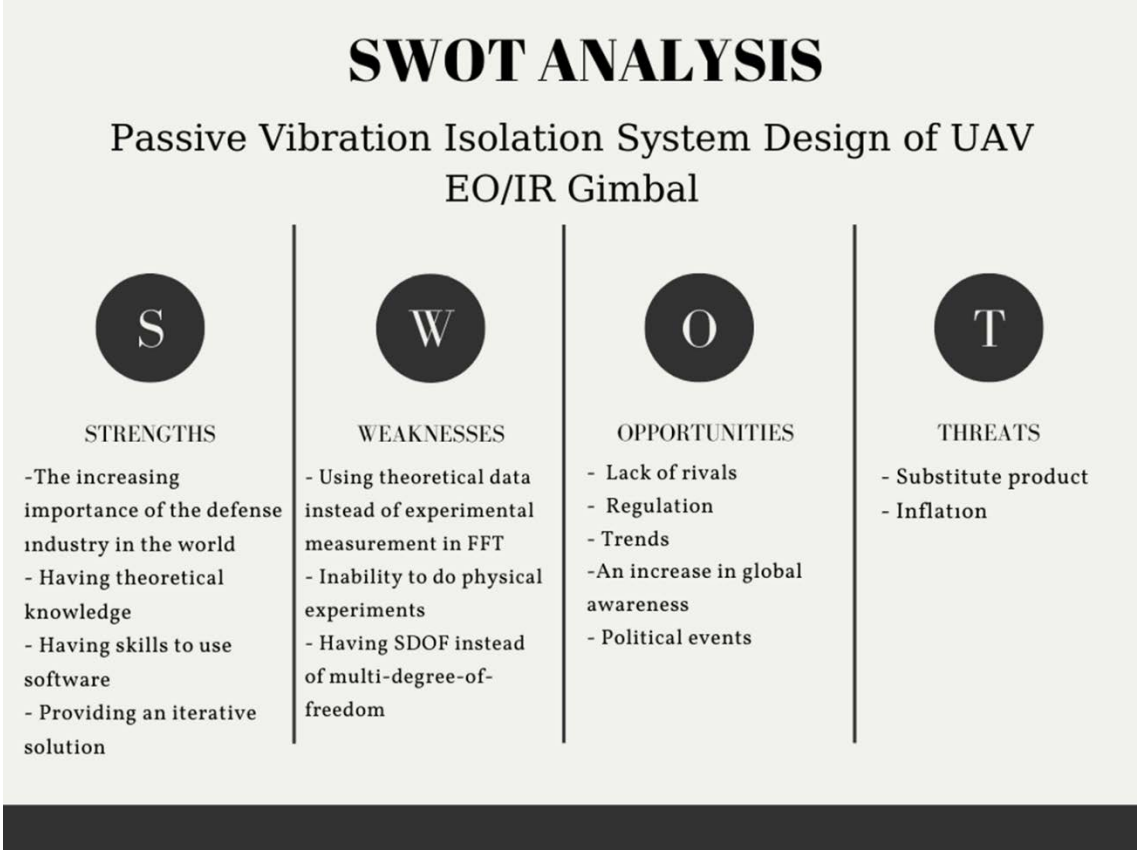

Figure 10.1 Swot analysis of project

Strengths are increasing importance of defence industry in the world, having theoretical knowledge, having skills to use software, and providing an iterative solution.

Weaknesses are using theoretical data instead of experimental measurement in FFT, inability to do physical experiments, and having SDOF design instead of multi-degree-of-freedom.

Opportunities are lack of rival, regulation, trends, increasing in global awareness, and political events.

Threats are substitute product, and inflation.

CONCLUSION AND FUTURE WORKS

1.25 Conclusions of the Current Work

In this undergraduate thesis, we designed a passive isolation system for the EO/IR Gimbal used in mini unmanned aerial vehicles by using the spring and damper, which are the basic mechanical isolation elements. While making this design, we followed an iterative method by using the necessary formulas for spring constant and damping coefficient selection. Then, to see the vibration damping after the k and c values found by the iterative method, we solved the quadratic non-homogeneous differential equation by hand and had it plotted from Matlab. Then we calculated this equation with Matlab differential equation solver code and compared it with the handwritten solution. As expected, the graphics were parallel. As seen in the graph, the vibration was damped in 0.8 seconds. In addition, we designed our gimbal in a CAD program considering design requirements such as dimension and mass. Then we subjected the drawn part to static analysis. Since the part exceeds the design requirements in mass, we lightened the part with topology optimization.

- After the topology optimization, the mass was reduced by approximately 15%.

After topology optimization, the final part design was subjected to modal analysis. Initially, the system's natural frequencies coincided with the base excitation frequency, and the system entered a state of resonance. In order to prevent this, we made some changes in the design of our piece, for example, by adding a rib, we moved the natural frequency values away from the base excitation frequency value.

- Third natural frequency increased from 92.8 Hz to 388.4 Hz.
- Fourth natural frequency increased from 104.2 Hz to 468.3 Hz.
- Fifth natural frequency increased from 186.7 Hz to 470.5 Hz

After reaching the desired natural frequency values, the analysis was performed in 3 different mesh sizes (5mm, 6mm, and 7mm) in order to observe the effect of mesh size on the results.

- A difference of less than 1% was observed in the frequency results obtained when the mesh number was increased.

Fortunately, the frequency values converge to a point as the mesh size decreases. This shows that the analysis is reasonable and acceptable.

As a result, the passive isolator system and gimbal design were made in accordance with the vibration that the gimbal in a mini unmanned aerial vehicle will be exposed to, and it validated with modal analysis was performed. Thus, it has been understood what the sources of vibration are, what methods can be damped and how changes can be made in the design so that the parts do not resonate, and it is hoped that it will guide future studies.

1.26 Recommendations for Future Works

- In future studies, more realistic results can be obtained from the harmonic vibration assumption made by us by experimentally performing vibration measurement and spectrogram analysis on the UAV.
- Afterward, the analyses made with a CAD design in which all optics and electronic parts, even nuts and gaskets, are modelled in the gimbal will be more useful in determining the natural frequencies and mode shapes.
- Finally, multi-degree-of-freedom in the system should be chosen instead of single-degree-of-freedom because it is more realistic.

.

REFERENCES

1. "Download MIL-STD-810H". Defense Logistics Agency, United States. 31 Jan 2019.
2. Al Nuaimi, O., Almelhi, O., Almarzooqi, A., Al Mansoori, A. A. S., Sayadi, S., & Swamidoss, I. (2018, October). Persistent surveillance with small Unmanned Aerial Vehicles (sUAV): a feasibility study. In Electro-Optical Remote Sensing XII (Vol. 10796, p. 107960K). International Society for Optics and Photonics.
3. Alsalaet, J. (2012). Vibration analysis and diagnostic guide. University of Basrah.
4. Al-Salti, N., Karimov, E., & Sadarangani, K. (2016). On a differential equation with Caputo-Fabrizio fractional derivative of order $1<\beta\leq 2$ and application to mass-spring-damper system. arXiv preprint arXiv:1605.07381.
5. Balaji, P. S., Moussa, L., Khandoker, N., Shyh, T. Y., Rahman, M. E., & Ho, L. H. (2017, July). Experimental study on vertical static stiffnesses of polycal wire rope isolators. In IOP Conference Series: Materials Science and Engineering (Vol. 217, No. 1, p. 012032). IOP Publishing.
6. Britannica, T. (2020). Editors of Encyclopaedia. Argon. Encyclopaedia Britannica.
7. Bursa, Ali İ. (2019). Motor bağlantı elemanlarının titreşim geçirgenliği üzerindeki etkilerinin incelenmesi (Master's thesis, Fen Bilimleri Enstitüsü).
8. Burström, L., Lindberg, L., & Lindgren, T. (2006). Cabin attendants' exposure to vibration and shocks during landing. Journal of sound and vibration, 298(3), 601-605
9. Carlson, H. (1978). Spring designer's handbook. Mechanical Engineering.
10. Choi, J. W., & Kwag, D. G. (2021). A Study on the Vibration Characteristics of EO/IR Gimbal for UAVs. Ilkogretim Online, 20(3).
11. controp , 'solutions', Acces: May 2022 https://www.controp.com/solutions/persistent-surveillance/
12. Dunno, K., & Batt, G. (2009). Analysis of in -flight vibration turbo propeller aircraft. Packaging Technology and Science: An International Journal, 22(8), 479-485.

13. Ellison, J., Ahmadi, G. and Kehoe, M. (2001). Passive vibration control of airborne equipment using a circular steel ring. Journal of Sound and Vibration. 246(1), 1-28.
14. endaq , Acces: May 2022 https://blog.endaq.com/vibration-analysis-fft-psd-and-spectrogram
15. European Patent, Patent No. US005184521A,1993
16. flir , 'aerial-kits' Acces: May 2022 https://www.flir.com/browse/industrial/aerial-kits/
17. Gebisa, A. W., & Lemu, H. G. (2017, December). A case study on topology optimized design for additive manufacturing. In IOP conference series: materials science and engineering (Vol. 276, No. 1, p. 012026). IOP Publishing.
18. Graham, K. S. (2000). Fundamentals of mechanical vibrations McGraw-Hill.
19. Harris, C. M., & Piersol, A. G. (2002). Harris' shock and vibration handbook (Vol. 5, pp. 1025-1083). New York: McGraw-Hill.
20. Hibbeler, R. C. (2005). Mechanics of materials. Pearson Educación.
21. Karaağaç, C. (2016). İHA Sistemleri Yol Haritası Geleceğin Hava Kuvvetleri 2016-2050. STM-Mühendislik Teknolojik Danışmanlık.
22. Kerwin, J. M. J. (2018). Selected Design Process Examples of a Two-Axis Gimbal System (Doctoral dissertation, The George Washington University).
23. Kumar, D. (2021). Durability Analysis of Helical Coil Spring in Vehicle Suspension Systems (Doctoral dissertation, Virginia Tech)
24. Kushwah, S., Parekh, S., Mistry, H., Bhatt, M., & Joshi, V. (2020). A Review Article on Design, Analysis and Comparative Study of Conventional and Composite Leaf Spring. IOSR Journal of Mechanical and Civil Engineering (IOSR-JMCE), 17(4).
25. Kuzey, N. B., & Yemenicioğlu, e. (2007). Istanbul Technical University Mechanical Engineering Faculty
26. Lai, Y. C., & Jan, S. S. (2011). Attitude estimation based on fusion of gyroscopes and single antenna GPS for small UAVs under the influence of vibration. GPS solutions, 15(1), 67-77.
27. Legriffon, I. (2016, August). Turbopropeller noise model assessment in CARMEN. In INTER-NOISE and NOISE-CON Congress and Conference

Proceedings (Vol. 253, No. 4, pp. 4227-4237). Institute of Noise Control Engineering.

28. Lengvarský, P., & Bocko, J. (2013). Theoretical basis of modal analysis. American Journal of Mechanical Engineering, 1(7), 173-179.
29. Liu, Y. (2020). Study on the vibrational comfort of aircraft in formation flight. Aircraft Engineering and Aerospace Technology.
30. Masterspring, ‘compression-spring-measurement-guide’ Acces: May 2022, URL: https://www.masterspring.com/resources/compression-spring-measurement-guide/
31. Min-Chie, C. H. I. U., Chang, Y. C., Long-Jyi, Y. E. H., & Chung, C. H. (2015). Numerical assessment of a one-mass spring-based electromagnetic energy harvester on a vibrating object. Archives of Acoustics, 41(1), 119-131.
32. Mokbel, H. F., Ying, L. Q., Roshdy, A. A., & Hua, C. G. (2012). Design optimization of the inner gimbal for dual axis inertially stabilized platform using finite element modal analysis. International Journal of Modern Engineering Research, 2, 239-244.
33. Nani, V. M., & Cireş, I. (2014). Vibration Control for Two Air Compressor Units Used in Tandem. World Journal of Engineering and Technology, 2(04), 314.
34. Sciulli, D. (1997). Dynamics and control for vibration isolation design (Doctoral dissertation, Virginia Polytechnic Institute and State University)
35. Shen, C., Fan, S., Jiang, X., Tan, R., & Fan, D. (2020). Dynamics Modeling and Theoretical Study of the Two-Axis Four-Gimbal Coarse–Fine Composite UAV Electro-Optical Pod. Applied Sciences, 10(6), 1923.
36. Singiresu, S. R. (1995). Mechanical vibrations. Boston, MA: Addison Wesley.
37. skypower , Acces: May 2022, https://skypower.online/produkt/sp-55-ts-ros/
38. smlease, ‘types-of-springs-and-their-app’ Acces: May 2022 https://www.smlease.com/entries/mechanism/types-of-springs-and-their-applications/
39. Sudhir Kaul - Modeling and Analysis of Passive Vibration Isolation Systems-Elsevier (2021)
40. Tewari, V. K., & Prasad, N. (1999). Three-DOF modelling of tractor seat-operator system. Journal of Terramechanics, 36(4), 207-219

41. threod, Acces: May 2022 https://threod.com/products/
42. Tomlin, M., & Meyer, J. (2011, May). Topology optimization of an additive layer manufactured (ALM) aerospace part. In Proceeding of the 7th Altair CAE technology conference (pp. 1-9).
43. Tse, F. S., Morse, I. E., & Hinkle, R. T. (1963). Mechanical vibrations. Boston: Allyn and Bacon.
44. uavfactory , 'penguin-b-uav' Acces: May 2022 https://uavfactory.com/en/penguin-b-uav
45. United State, Patent No. US005184521A,1993
46. United State, Patent No. US10260591B2,2019
47. United State, Patent No. US11216013B2,2022
48. United State, Patent No. US1955770,1933
49. United State, Patent No. US2017175948A1,2017
50. United State, Patent No. US2020307826A1,2020
51. United State, Patent No. US2020307826A1,2020
52. United State, Patent No. US3638502,1972
53. United State, Patent No. US6263160,2001
54. United State, Patent No.US1634950,1923
55. Wang, Y., Zheng, L., Gao, Y., & Li, S. (2020). Vibration Signal Extraction Based on FFT and Least Square Method. IEEE Access, 8, 224092-224107.
56. Warnotte, V., Stoica, D., Majewski, S., & Voiculescu, M. (2007). State of the art in the pounding mitigation techniques. INTERSECTII/INTERSECTIONS, 4(3)
57. Weimin, C., Gang, L., & Wei, C. (1997). Research on ring structure wire-rope isolators. Journal of materials processing technology, 72(1), 24-27.
58. World Intellectual Property Organisation, Patent No. 9765925,2015
59. World Intellectual Property Organisation, Patent No. WO1998016871A1,1998

APPENDICES

Appendix 1 ‘Transmissibility vs r’ graph

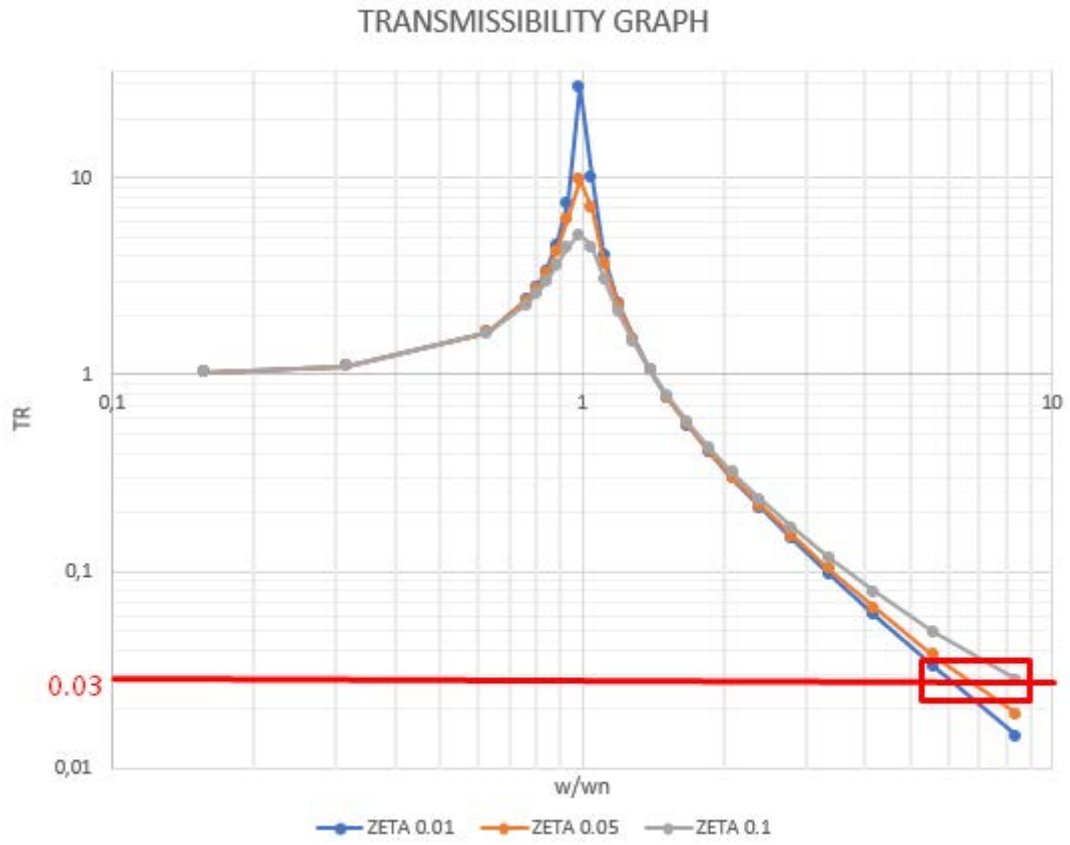

Appendix 2 ‘Transmissibility vs r’ graph zoomed

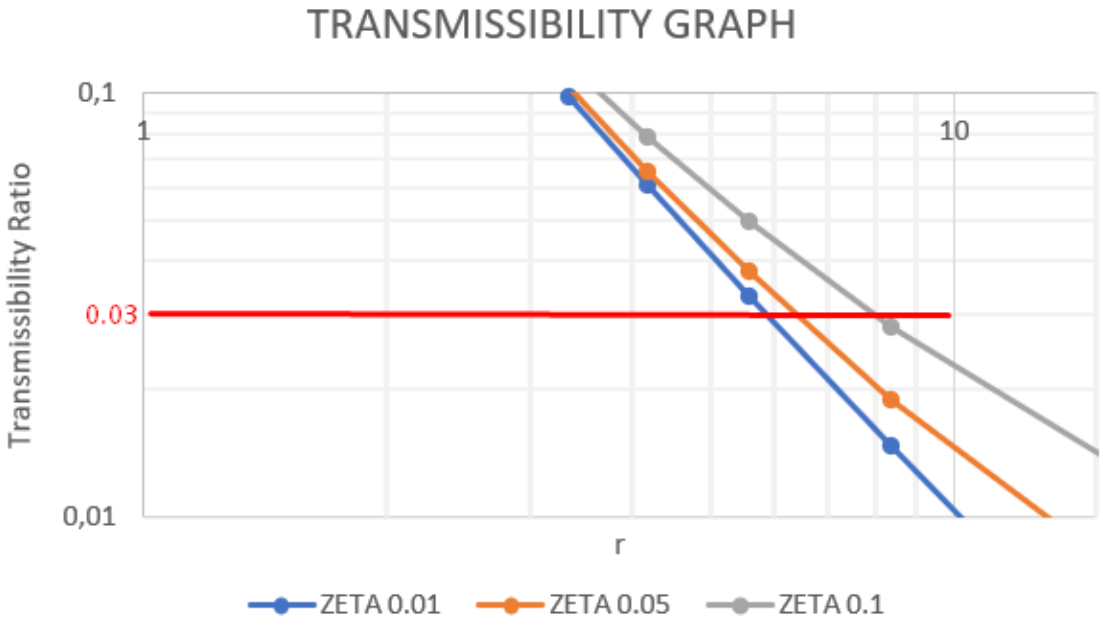

Appendix 3 Matlab code to solve differential equation

```
clear all
clc
syms y(x)
y_dot = diff(y);
ode =1.5* diff(y,x,2)+20*diff(y,x)+50000*y
==500*sin(1256.64*x);
cond1 = y(0) == 2*10^-4;
cond2 = y_dot(0) == -10^-3;
conds = [cond1 cond2];
ySol(x) = dsolve(ode,conds);
ySol = simplify(ySol)
pretty(ySol)
x=0:0.01:2 ;
plot(x,ySol(x))
```

Appendix 4 Final design render photo